Doctoral Dissertations and Master's Theses

Spring 4-2016

Nonlinear Control of a Thermoacoustic System with Multiple Heat Sources and Actuators

Mikael O. Molina Sandoval
Embry-Riddle Aeronautical University

Follow this and additional works at: https://commons.erau.edu/edt

Part of the Aerospace Engineering Commons, and the Engineering Physics Commons

NONLINEAR CONTROL OF A THERMOACOUSTIC SYSTEM WITH MULTIPLE HEAT SOURCES AND ACTUATORS

BY

MIKAEL O. MOLINA SANDOVAL

A Thesis

Submitted to the Department of Physical Sciences

and the Committee on Graduate Studies

In partial fulfillment of the requirements

for the degree of

Master in Science in Engineering Physics

04/2016

Embry-Riddle Aeronautical University

Daytona Beach, Florida

NONLINEAR CONTROL OF A THERMOACOUSTIC SYSTEM WITH MULTIPLE HEAT SOURCES AND ACTUATORS
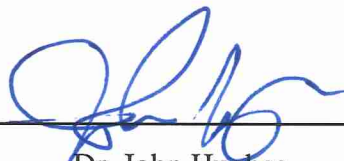
by

Mikael O. Molina Sandoval

This thesis was prepared under the direction of the candidate's Thesis Committee Chair, Dr. Mahmut Reyhanoglu, Professor, Daytona Beach Campus, and Thesis Committee Members Dr. John Hughes, Associate Professor, Daytona Beach Campus, and Dr. William Mackunis, Assistant Professor, Daytona Beach Campus, and has been approved by the Thesis Committee. It was submitted to the Department of Physical Sciences in partial fulfillment of the requirements of the degree of
Master of Science in Engineering Physics
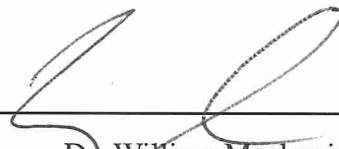
THESIS COMMITTEE:

_____
Dr. Mahmut Reyhanoglu,
Committee Chair

_____   _____
Dr. John Hughes,   Dr. William Mackunis,
Committee Member   Committee Member

_____   _____
Dr. Terry Oswalt,   Dr. William Grams,
Department Chair, Physical Sciences   Dean, College of Arts and Sciences

_____
Dr. Christopher Grant,
Associate Chancellor

iii

Acknowledgments

First and foremost, I would like to thank my thesis advisor Dr. Mahmut Reyhanoglu from Embry-Riddle Aeronautical University for initially suggesting the area of work for this thesis and always being available for support. While allowing this thesis to be my own work, he often gave me the necessary push to continue my work and steered me in the right direction whenever he thought I needed it.

I would also like to thank my previous advisor Dr. Matthew Zettergren, whom I worked with for several semesters before starting this thesis. While his work did not directly affected the development of my current research, he was able to teach me some of the necessary skills that I applied during this work. For that I am very much grateful.

Additionally, I thank my committee members: Dr. John Hughes and Dr. William Mackunis for being part of the validation of this research project. This could not have been conducted without their input.

To all my friends whom I have shared a sleepless night before deadlines and encouraged me to keep pushing forward. Thanks for all the fun times, because hard work has to always be followed by some kind of leisure, which was often provide by you.

Finally, I must also express my gratitude to my parents and my sisters for providing

me the necessary support, and continuous encouragement during my years of study and researching. This gave me the fortitude to finish my undergraduate studies and go on to my graduate studies. This accomplishment would not have been possible without them.

Thank you,

Mikael O. Molina Sandoval

Abstract

Thermoacoustic instabilities can occur in thermal devices when unsteady heat release is coupled with pressure perturbations. This effect results in excitation of eigen-acoustic modes of the system. These instabilities can lead to unpredictable behavior of the system. Gas-turbine combustion systems are especially prone to this phenomenon reducing their overall efficiency. Additionally, due to the nature of the combustion, the turbines end up releasing undesired amounts of harmful chemicals to the atmosphere, such as Nitrous Oxide (NOX).

A Rijke tube, representing a resonator with a mean flow and a concentrated heat source, is a convenient system to study the thermoacoustic phenomena. Under certain conditions of the main system, a loud sound is generated through a process similar to that in devices prone to thermoacoustic instabilities. Rijke devices have been extensively studied and several models which provide accurate representation of the system, already exist. These models often assume that the system is compromised of a single heat source which drives the instability. This may not be the case as combustors which use more than one flame are common for engines and industrial burners. By using the aforementioned models, a nonlinear feedback control scheme is developed for a Rijke-type combustion system with

n actuators and *m* heat sources.

The performance of the controller is tested under different scenarios, assuring that it is capable to exponentially stabilize the system despite any nonlinearities present in the heat release. Additionally, active control is studied in detail by analyzing the impact of the control parameters under different positioning of heat sources. The effect of the location for the actuators is also studied.

Contents

List of Tables

List of Figures

Chapter 1

INTRODUCTION

With the demand for higher efficiency machines for production of electricity, gas turbines have replaced other forms of combustion engines in various types of vehicles. In addition, the development of mini gas turbine technology has become a solution for heat and power in many households and businesses. These turbine engines offer a high efficiency (60%) along with low maintenance requirements [Annaswamy (2000)]. It is known however, that at higher temperatures ($1500^{o}C$), these combustion engines begin to emit pollutants harmful to the human health, particularly Nitrous Oxide (NOX).

Following the threshold of $1500^{o}C$, any rise in temperature causes a rapid increase of thermal NOX creation rate [Schefer (2003)]. This problem is often prevented by reducing the maximum flame temperature or preventing hot spots with the use of coolants or lean premixed air and fuel streams. The use of coolants simply complicates the design of the already complex gas turbine engine; and lean premixed combustion is known to have other serious issues, such as flow reversal [Culick (1988)].

A type of combustion reaction is classified depending on where the fuel and air are

mixed (either before the combustion chamber, or in the chamber itself). While premixed combustion offers certain advantages, it may be dangerous if certain conditions are violated. Often, these types of combustion systems are prone to high amplitude pressure perturbations, which can damage the turbine and may cause it to fail [Correa (1988)]. Gas turbines usually use a partially premixed approach instead. These premixed flames normally have a high response time, which causes them to couple with a low acoustic frequencies. Nevertheless pressure perturbations are eventually significant. These pressure perturbations and coupling can result in thermoacoustic instabilities.

1.1 Thermoacoustic Instability

Thermoacoustic instabilities refer to the appearance of pressure and velocity oscillations within a fluid coupled with some unsteady heat release. These kinds of instabilities are often found in systems whose heat release is coupled with pressure or velocity disturbances. Combustion systems are often associated with these instabilities due to favorable acoustic properties combined with a relatively high heat release. Figure 1.1 provides a representation of the positive feedback loop that destabilizes the system.
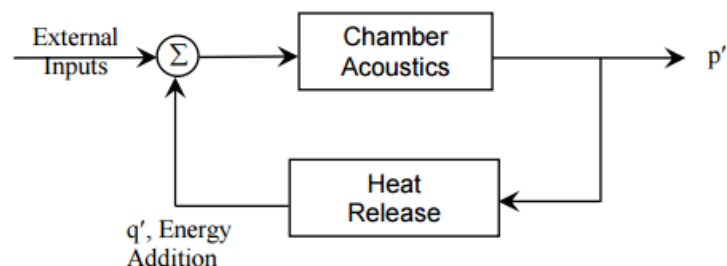
Figure 1.1: Feedback loop of a thermoacoustic instability [Matveev (2003)].

Essentially, the instabilities are self-sustained large amplitude oscillations of pressure

and velocity with the flame acting as an acoustic actuator and the combustions chamber as an acoustic resonator. The occurrence of combustion instability depends on the phase between the heat release and pressure fluctuations at the heat source.

The first known study of this phenomena was performed by Rijke during the 19th century. However, there were several reports of sound interaction with flames, sound being generated by glass workers as they blew molten glass bulbs or other forms of sound-heat release interaction.

1.2 Rijke Tube

Studying thermoacoustic instabilities requires a complex analysis of an already complicated phenomenon. In 1859, Petrus Rijke, a Dutch physicist, discovered a way to produce sound using heat through a simple device. This mechanism was named the Rijke tube: it consisted of a vertical pipe with a gauze located in the lower half of the tube. If the gauze was heated to a high enough temperature, the pipe would generate a high-intensity tone. This was one of the earliest studies of thermoacoustic instabilities. Figure 1.2 shows a diagram of the mechanism.

The most important component is the heat source and its positioning. If the heat gauze has a high enough temperature, its location is on the bottom half of the tube, and a mean flow is present due to natural convection; the device is able to create standing pressure waves. This type of thermoacoustic instability creates a frequency of sound related to the acoustic eigenmodes of the tube [Juniper (2010)].

The process was thoroughly explained by Lord Rayleigh. During the first half of the
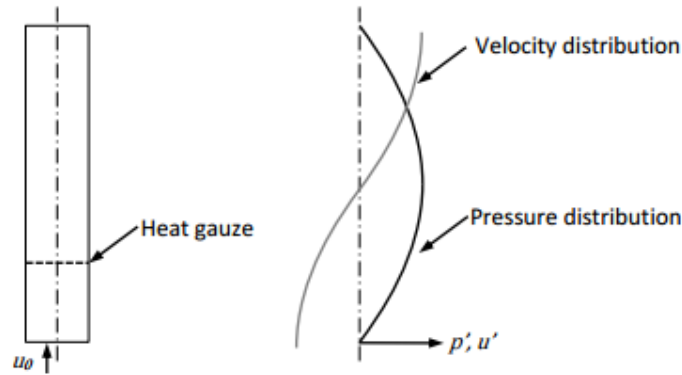
Figure 1.2: Rijke tube and the approximate velocity and pressure distributions [Matveev (2003)].

perturbation, the combined effect of mean flow and the acoustic velocity pushes the cold gas through the gauze. When the gas is heated, its density changes and it becomes an acoustic source. When the velocity is reversed, the hot gas passes through the gauze again which reduces the temperature difference and lowers the heat transfer. This lowered heat transfer cools the fluid located higher than the gauze, and the process repeats itself indefinitely [Yang et al. (2015)].

1.3 Motivation

As mentioned before, Rijke tubes are not the only source of thermoacoustic oscillations. These instabilities are often observed in rocket engines, furnaces, and previously mentioned, gas turbines.

Thermoacoustic instability plays important roles in technical applications. Uncontrolled large amplitude oscillation created by the combustion system may lead to larger pressure load, unexpected or uncontrolled heat transfer, undesired chemical reactions, or in the worst case, failure of the system. Designers often go through great lengths to prevent

the appearance of said instabilities, to ultimately avoid its possible negative effects.

A common and simple approach is the iterative design of a stable combustion through the use of empirical data. These tests are often expensive and time consuming. The data is also only applicable to a single type of system. The characterization of small or medium scale laboratory flames is generally more accessible. This approach is often used to create flame models for industrial burners.

The most common approach for modeling these kinds of systems uses a combination of 1D fluid equations coupled with heat release; normally represented in the energy balance equation. Due to the complexity, these equations are often reduced to a simplified model fit for the system. This simplification allows for a numerical model to be developed as well as an approximate analytical solution. These models tend to be specific to the problem, although some generalization can be applied to simple systems.

Following the simplification of the system, several control techniques can be attempted to prevent these instabilities. Passive solutions are often used through the installation of Helmholtz resonators or cavities in the combustion chamber. Multiple injection ports for fuel is a more advanced method as it requires clever positioning and timing. Nevertheless, sometimes these passive solutions are not enough and active control theory may be required to prevent the growth of pressure oscillations.

Through the use of sensors and actuators, a control mechanism can be installed in the combustion chamber. Through the use of actuators, the controller can modulate several properties of the system based on sensor readings. Modulating the pressure waves or the fuel flow can be done to prevent any transient growth. An example of active control can be seen in Figure 1.3.
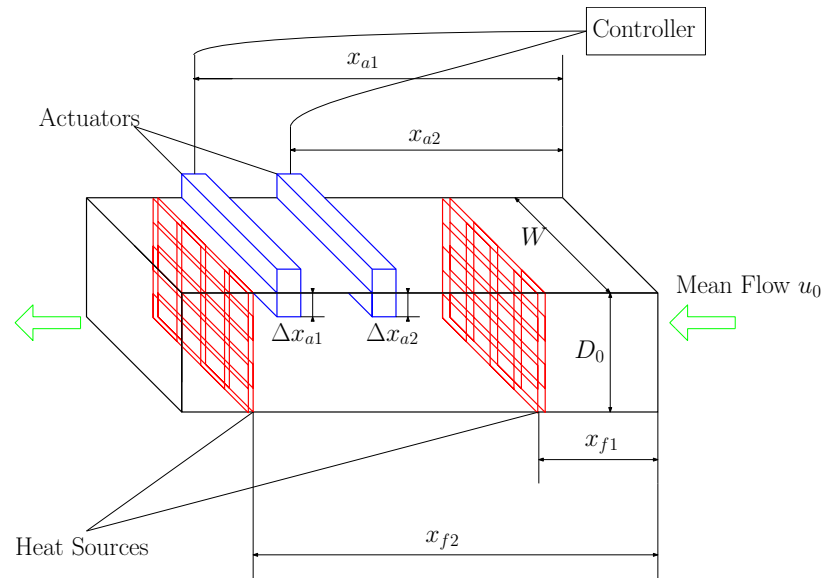
Figure 1.3: A Rijke-like system with two actuators and two heat sources.

1.4 Objective

The main objectives of this thesis are stated as follows:

- To derive a mathematical model that incorporates heat transfer analysis, appropriate boundary conditions, multiple heat sources, and is capable of showing nonlinear transient growth characteristic of a Rijke system.

- Simplify said model, such that it can be expressed in a non-dimensional form.

- Show the evolution of an uncontrolled thermoacoustic system.

- Investigate the effect of the placement of different heat sources.

- Develop a nonlinear control technique that reduces aforementioned transient growth. Furthermore, the nonlinear control parameters must be valid for a realistic scenario.

The outline of the thesis is shown as follows: Chapter 2 is dedicated to the development of the mathematical model. The assumptions are listed and explained in detail, along with

the initial and boundary conditions of the system. This continues with the derivation of the acoustic equations based on our initial fluid conservation equations. Different control techniques are explored in Chapter 3. Finally, the last portion of the chapter is dedicated to the development of the nonlinear control model. Chapter 4 explores the results from simulations with control techniques applied to the mathematical model. Different scenarios are considered and throughly analyzed. Any apparent inconsistency is explored in detail. Chapter 5 concludes all the work done and offers suggestions for future work.

Chapter 2

MATHEMATICAL MODEL

2.1   Objectives and Assumptions

The main objective of this chapter is to develop a mathematical model that approximately

describes the natural behavior of a Rijke tube. The development of a controller based on

the model is later studied Chapter 3. There have been several studies on thermoacoustic

instabilities in Rijke system. The models are constructed following the objectives of the

authors, simplifying the dynamic model to a more convenient form; while still retaining

retaining the concept of a Rijke system. For the system studied in this thesis, a general set

of guidelines can be followed from the work found in [Matveev (2003)]. The following are

the assumptions used for the derivation of the mathematical model:

(a) All time-averaged properties of an airflow are treated as constants along the duct.

(b) All heat release is transmitted to the air flow from the heat sources. Heat conduction

    to structural elements and thermal radiation are ignored.

(c) The system is a one-dimensional horizontal Rijke-like thermoacoustic duct. Thus, all waves are planar and any viscous or thermal boundary layer is ignored.

(d) Any variation of the system is assumed to be a small disturbance. Any second order terms are then assumed to be small and can be neglected.

(e) Gravity and other body forces are ignored.

(f) Mean gas flow speed is small compared to the speed of sound.

(g) The thickness of the heat sources is small compared to the acoustic wavelength, such that it can be represented as a dirac delta function.

(h) The actuators can be treated as point sources, such that their effect is at a specific point in the tube.

Assumption (a) refers to values such as temperature of the system, specific heat, thermal diffusivity, etc. These values are not directly affected by the governing equations and are treated as constants through the tube. Assumption (c) indicates the absence of boundary layers, the system does not have a way to dissipate energy (Through the derivation we learn that boundary conditions do not permit acoustic dissipation to surroundings). This is solved by adding a damping parameter studied later in this chapter.

2.2 Deriving a Thermoacoustic Model

As with any perfect gas, the analysis can start from the fluid conservation equations. As shown in [Landau and Lifshitz (1959)], the fluid mass, momentum and energy equations

are given by:

$$\frac{\partial \rho}{\partial \widetilde{t}} + \triangledown \cdot (\rho \vec{u}) = \rho \Omega, \tag{2.1}$$

$$\frac{\partial \rho \vec{u}}{\partial \widetilde{t}} + \triangledown \cdot (\rho \vec{u} \cdot \vec{u}) = -\triangledown p + \rho \vec{B} + \triangledown \cdot \tau, \tag{2.2}$$

$$\frac{\partial p}{\partial \widetilde{t}} + \vec{u} \cdot \triangledown p = -\gamma p \triangledown \cdot \vec{u} + (\gamma - 1)\dot{Q} + \rho a^2 \Omega + \gamma \dot{Q}_a \tag{2.3}$$

where $\vec{u}$ is the velocity vector of the fluid, ρ is the density of the fluid, and p is the pressure. Additionally, γ represents the specific heat ratio; B is the specific body force; τ is the viscous stress tensor; $\dot{Q}$ is the heat addition rate per unit volume. This heat source will be defined later in the chapter, it is left as a general heat source for the main derivation. Ω is the volumetric source intensity per unit volume. $\dot{Q}_a$ is the actuation signal; this term is added as shown in [Fleifil (2007)]. The energy equation (2.3) is written in such a way that it neglects heat conduction and thermal radiation.

We can further reduce the equations by considering the gas to be inside the duct beyond the outer edge of the boundary layers formed at the duct walls so that viscous stress can be ignored. Volumetric source intensity is assumed to be zero. As explained in Section 2.1, body forces are also ignored. To create a homogeneous and one-dimensional velocity profile, we apply the assumption that the boundary layer is significantly smaller than the diameter of our tube. We then formulate our problem with respect to the x-axis, aligned with our mean flow and such that our velocity vector u simplifies to its x component. Given

these assumptions, equations (2.1)-(2.3) become:

$$\frac{\partial \rho}{\partial \tilde{t}} + \frac{\partial}{\partial \tilde{x}}(\rho u) = 0, \tag{2.4}$$

$$\frac{\partial \rho u}{\partial \tilde{t}} + \frac{\partial}{\partial \tilde{x}}(\rho u^2) = -\frac{\partial p}{\partial \tilde{x}}, \tag{2.5}$$

$$\frac{\partial p}{\partial \tilde{t}} + u\frac{\partial p}{\partial \tilde{x}} + \gamma p\frac{\partial u}{\partial \tilde{x}} = (\gamma - 1)\dot{Q} + \gamma\dot{Q}_a \tag{2.6}$$

Here, $\tilde{t}$ and $\tilde{x}$ represent the dimensional time and space respectively. To further reduce our equations, pressure, heat addition, the actuation signal, density and velocity can be represented as sums of a constant in time (denoted by subscript 0), and a small amplitude wave or a small disturbance (denoted by a tilde):

$$\rho(\tilde{x},\tilde{t}) = \rho_o + \tilde{\rho}(\tilde{x},\tilde{t}) \tag{2.7}$$

$$p(\tilde{x},\tilde{t}) = p_o + \tilde{p}(\tilde{x},\tilde{t}) \tag{2.8}$$

$$u(\tilde{x},\tilde{t}) = u_o + \tilde{u}(\tilde{x},\tilde{t}) \tag{2.9}$$

$$\dot{Q}(\tilde{x},\tilde{t}) = \dot{\tilde{Q}}(\tilde{x},\tilde{t}) \tag{2.10}$$

$$\dot{Q}_a(\tilde{x},\tilde{t}) = \dot{\tilde{Q}}_a(\tilde{x},\tilde{t}) \tag{2.11}$$

Applying a small amplitude approximation: any second order term or product between disturbances can be considered zero. By substituting equations (2.7)-(2.11) into equations

(2.4)-(2.6) a simplified set of fluid conservation equations can be obtained:

$$\frac{\partial \widetilde{\rho}}{\partial \widetilde{t}} + u_o \frac{\partial \widetilde{\rho}}{\partial \widetilde{x}} + \rho_o \frac{\partial \widetilde{u}}{\partial \widetilde{x}} = 0, \tag{2.12}$$

$$\rho_0 \frac{\partial \widetilde{u}}{\partial \widetilde{t}} + \frac{\partial \widetilde{p}}{\partial \widetilde{x}} = 0 \tag{2.13}$$

$$\frac{\partial \widetilde{p}}{\partial \widetilde{t}} + \zeta \frac{c_0}{L_0} \widetilde{p} + \gamma p_0 \frac{\partial \widetilde{u}}{\partial \widetilde{x}} = (\gamma - 1)\dot{\widetilde{Q}} + \gamma \dot{\widetilde{Q}}_a \tag{2.14}$$

Due to the nature of our problem, equation (2.12) can be ignored. It provides information of the density of the fluid, based on the velocity. It is reassuring to know the problem is not ignoring any density fluctuations; however the velocity and pressure can be independently calculated through the use of equations (2.13)-(2.14) without solving for density.

For the system examined, the boundary conditions do not allow the dissipation of acoustic energy by doing work to the surroundings. Normally, the system is able to dissipate energy through the viscous and thermal boundary layer. However, the waves are approximated to be planar, which dismisses the interaction of the fluid with the tube walls. Because of this, an additional damping term is added to equation (2.14). This term is dependent on the pressure fluctuations of the system and is accompanied by the damping parameter ζ. Further explanation of this can be found in [Juniper (2010)] derived from correlations between [Matveev (2003)] and [Landau and Lifshitz (1959)].

With equation (2.13) there is a direct relation between the time derivative of velocity and spatial derivative of pressure; this is called the acoustic momentum equation. Equation

(2.14) refers to the energy balance of the system, this is called the acoustic energy equation. Furthermore, we can define our heat transfer and actuation signal as follows:

$$\dot{\tilde{Q}} = \sum_{g=1}^{G} \dot{\tilde{Q}}_{sg} \widetilde{\delta}(\widetilde{x} - \widetilde{x}_{fg}) \tag{2.15}$$

$$\dot{\tilde{Q}}_a = \sum_{k=1}^{K} \alpha_{ak} \widetilde{v}_{ak} \widetilde{\delta}(\widetilde{x} - \widetilde{x}_{ak}) \tag{2.16}$$

For equation (2.16), α_{ak} represents the ratio between the cross-sectional area of the kth actuator (S_k) to the cross-sectional area of the tube (S). Both the gth heat sources and kth actuator are located at x_{fg} and x_{ak} respectively. They are treated as point sources, as shown by the presence of the delta function.

As stated in 2.1, the heat sources can be assumed to be small enough to be represented as delta functions. Additionally, it is modeled after King's law [Yang et al. (2015)]:

$$\dot{\tilde{Q}}_{sg} = \mathscr{K}_g \left[\sqrt{\left| \frac{u_0}{3} + \widetilde{u}_f \left(\widetilde{t} - \widetilde{\tau}_g \right) \right|} - \sqrt{\frac{u_0}{3}} \right] \tag{2.17}$$

The time delay is represented by $\widetilde{\tau}_g$ and is different for each flame. The step function is used to simulate the processes of heat transfer and thermal diffusion between the heated wire and the gas. Note that the subscript g denotes a different heater. The $\mathscr{K}_g$ coefficient is dependent on the qualities of the heater and can be calculated with the following formula:

$$\mathscr{K}_g = \frac{2L_{wg}(T_{wg} - T_0)}{\sqrt{3}S} \sqrt{\pi \lambda c_v \rho_0 \frac{d_{wg}}{2}} \tag{2.18}$$

where d_{wg}, L_{wg} and T_{wg} denote the diameter, length and temperature of the heated wire.

The different actuators are denoted by the subscript k, α_{ak} describes the ratio of the cross-

sectional area S_{ak} of the kth actuator to the area of the duct S. As explained in [Fleifil

(2007)], the acoustic dynamics and energy transfer of a monopole-like sound source can be

modeled as:

$$\widetilde{v}_{ak} = \mathscr{R}_k \frac{\widetilde{u}(\widetilde{x}_{ak})}{u_0} + \mathscr{S}_k \frac{\widetilde{p}(\widetilde{x}_{ak})}{\gamma M_0 p_0} \tag{2.19}$$

where $\mathscr{R}_k$ and $\mathscr{S}_k$ are our dimensional control parameters. M_0 is the Mach number which

is assumed to be low.

2.3   Formulation of Nondimensional Thermoacoustic System

In order to further simplify our control problem, our equations can be put in a nondimen-

sional form. Any variable with a tilde can be replaced by one of the following:

$$u = \frac{\widetilde{u}}{u_0}, \qquad p = \frac{\widetilde{p}}{\gamma M_0 p_0}, \qquad \dot{Q}_s = \frac{\dot{\widetilde{Q}}_s}{\gamma p_0 u_0}$$

$$x = \frac{\widetilde{x}}{L_w}, \qquad t = \frac{\widetilde{t} c_0}{L_w}, \qquad \delta(x - x_f) = \frac{\widetilde{\delta}(\widetilde{x} - \widetilde{x}_f)}{L_0} \tag{2.20}$$

Constants used to nondimensionalize the system include: the mean flow u_0, the mach num-

ber M_0, mean pressure p_0, the length of the duct L_0, and speed of sound c_0. As such,

equations (2.13)-(2.14) are reduced to their respective non-dimensional forms following:

$$\frac{\partial u}{\partial t} + \frac{\partial p}{\partial x} = 0 \tag{2.21}$$

$$\frac{\partial p}{\partial t} + \zeta p + \frac{\partial u}{\partial x} = (\gamma - 1) \sum_{g=1}^{G} \dot{Q}_{sg} \delta(x - x_{fg}) + \gamma \sum_{k=1}^{K} \alpha_{ak} v_{ak} \delta(x - x_{ak}) \tag{2.22}$$

Note that the heat transfer parameter and the actuation signal have changed to the following:

$$\dot{Q}_{sg} = \mathscr{K}_g \left[\sqrt{\left| \frac{1}{3} + u_{fg}(t - \tau_g) \right|} - \sqrt{\frac{1}{3}} \right] \tag{2.23}$$

$$\mathscr{K}_g = \frac{2L_{wg}(T_{wg} - T_0)}{\sqrt{3u_0} S \gamma p_0} \sqrt{\pi \lambda c_v \rho_0 \frac{d_{wg}}{2}} \tag{2.24}$$

$$v_{ak} = \mathscr{R}_k u(x_{ak}) + \mathscr{S}_k p(x_{ak}) \tag{2.25}$$

Following the work of [Culick (1988)], a Galerkin approximation can be used to transform the partial differential equations into a set of coupled ordinary differential equations (ODEs). This method implies that the final result for pressure and velocity is a superposition of waves. The amplitude of the modes are represented by the product of a time-dependent function $\eta_j(t)$ and a spatially dependent trigonometric function $v_j(x)$ [Wang (1972)].

The solution for the velocity u can be expressed as:

$$u(x,t) = \sum_{j=1}^{N} v_j(x) \eta_j(t) \tag{2.26}$$

This solution has to satisfy the previously stated boundary conditions ($\frac{\partial u}{\partial x} = 0$). As such,

$v_j(x)$ can be written as a trigonometric function, whose frequency is $\omega_j = \frac{j\pi}{L_0}$. Note however, that our system is nondimensional, so $L_0 = 1$:

$$u(x,t) = \sum_{j=1}^{N} \cos(j\pi x)\eta_j(t) \tag{2.27}$$

Using equation (2.13), we can obtain a relationship for the pressure:

$$p(x,t) = -\sum_{j=1}^{N} \frac{\sin(j\pi x)}{j\pi}\dot{\eta}_j(t) \tag{2.28}$$

Empirical proof of existence of the waves described by Equations (2.27)-(2.28) can be found in [Epperlein et al. (2014)]. Applying the solutions for pressure and velocity to equation (2.14), allows us to obtain the following ODE:

$$\frac{\ddot{\eta}_j}{j\pi} + j\pi\eta_j + \zeta_j\frac{\dot{\eta}_j}{j\pi} = -2(\gamma-1)\sum_{g=1}^{G}\dot{Q}_{sg}(x_{fg},t-\tau_g)\sin(j\pi x_{fg})$$

$$-2\gamma\sum_{k=1}^{K}\alpha_{ak}V_a(x_{ak},t)\sin(j\pi x_{ak}) \tag{2.29}$$

In this form, a specific value for the damping parameter ζ_j can obtained for each mode [Rubio-Hervas et al. (2015)]. This coefficient is referred as the thermo-viscous damping coefficient, [Landau and Lifshitz (1959)] and its value is dependent on the natural mode of the wave, such that:

$$\zeta_j = c_1 j^2 + c_2 j^{0.5} \tag{2.30}$$

With the constants c_1 and c_2 being the same for each mode. The value of these are derived

experimentally [Juniper (2010)].

One of the main objectives of the controller is to prevent triggering [Fleifil (2007)] or initial growth of the instability. This triggering can be observed with the acoustical energy per cross-sectional area of the system. This energy has two components given by the kinetic energy and potential energy, expressed in terms of the velocity and the pressure of the fluid respectively. The integral over the acoustic length, will give the total acoustical energy of the fluid such that $E(t)$ is given by:

$$E(t) = \frac{1}{2} \int_0^1 \left(p^2(x,t) + u^2(x,t) \right) dx \tag{2.31}$$

Substituting the solutions given by equations (2.27)-(2.28), we can obtain the following:

$$E(t) = \frac{1}{2} \int_0^1 \left(\left(-\sum_{j=1}^{N} \frac{\sin(j\pi x)}{j\pi} \dot{\eta}_j(t) \right)^2 + \left(\sum_{j=1}^{N} \cos(j\pi x) \eta_j(t) \right)^2 \right) dx \tag{2.32}$$

We can use orthogonality to indicate that $\int_0^1 \left(\sin(i\pi x) \sin(j\pi x) \right) dx = 0$ if $i \neq j$ which allows us to cancel any cross terms that originate from squaring the sum. Additionally, $\int_0^1 \left(\sin(i\pi x) \sin(j\pi x) \right) dx = 1$ if $i = j$, which further simplifies the integral to:

$$E(t) = \frac{1}{2} \left[\sum_{j=1}^{N} \left(\frac{\dot{\eta}_j(t)}{j\pi} \right)^2 + \sum_{j=1}^{N} \left(\eta_j(t) \right)^2 \right] \tag{2.33}$$

Furthermore, we can represent an energy ratio written in terms of the initial energy of the system:

$$G(t) = \max_{E(0)} \frac{E(t)}{E(0)} \tag{2.34}$$

The initial value is always 1 such that any growth after $t = 0$ can be generally attributed to the triggering of the system, such that when $\max_t G(t) > 1$ a transient growth is occurring, and if $\max_t G(t) < 1$, the system is exponentially decaying.

2.4 Results from the Model

For this section, an uncontrolled case is studied in the presence of two heat sources. The purpose of this section is to determine whether or not the model is accurate enough. The parameters shown in Table 2.1 were used for the simulation. The triggering disturbance is a low frequency wave in the velocity profile. The initial pressure of the system does not contain a disturbance.

Table 2.1: Parameters for testing the mathematical model.

List of Parameters			
Parameter	Value	Parameter	Value
ρ	$1.025\frac{\text{kg}}{\text{m}^3}$	λ	$0.0328\frac{\text{m}^2}{\text{s}}$
c_v	$719\frac{\text{J}}{\text{kgK}}$	γ	0.4
L_0	1m	T_b	295K
c	$344.64\frac{\text{m}}{\text{s}}$	u_0	$2.5\frac{\text{m}}{\text{s}}$
L_w	$2.5m$		
d_{w1}	0.5×10^{-3}m	d_{w2}	0.5×10^{-3}m
T_{w1}	1800K	T_{w2}	1800K
x_{f1}	0.625m	x_{f2}	1m
τ_1	100ms	τ_2	500ms
P_0	8.69×10^4Pa	S_c	1.56×10^{-3}m^2
c_1	0.04	c_2	0.004

From the works of [Fleifil (2007)], we expect to see a transient growth followed by an energy ceiling. This ceiling is given by a balance between the energy dissipation caused by the thermo-viscous damping, and the energy gained from the heaters. Additionally, King's

law is not approximated to a linear function, as it is in [Juniper (2013)]; therefore, there

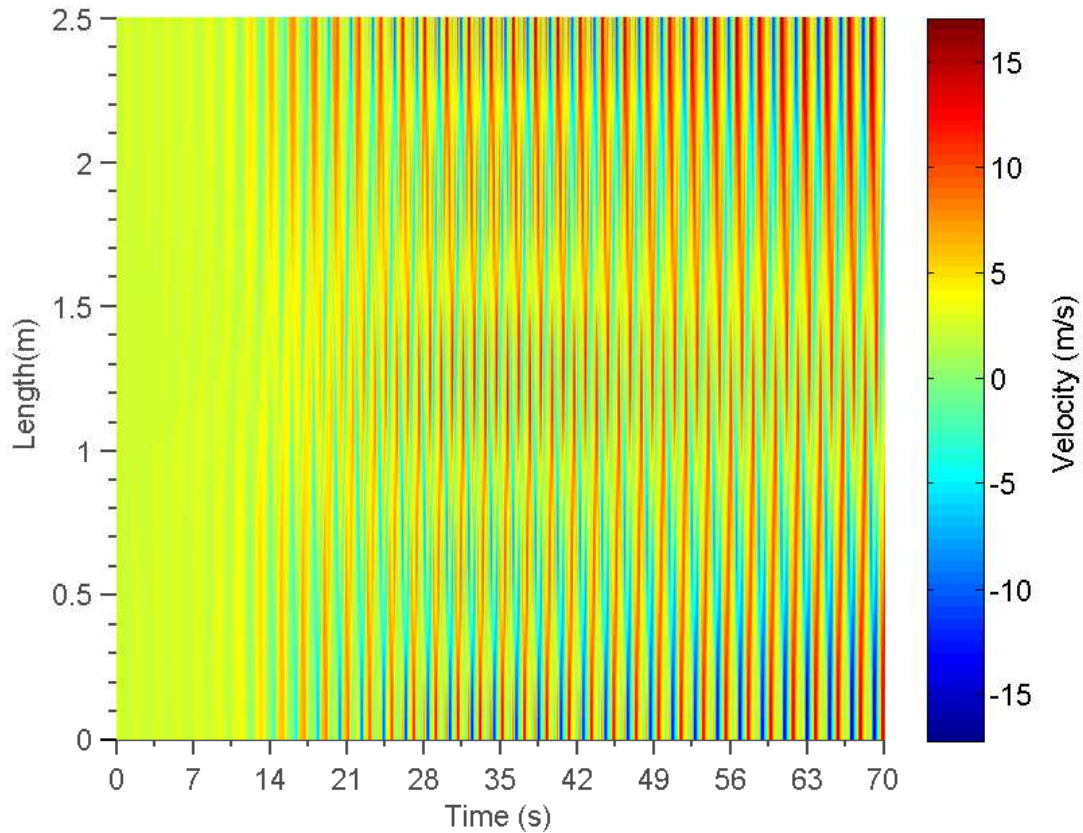should not be any decay after a large time has passed.

Figure 2.1: Contour plot of velocities along the Rijke-tube.

Figure 2.1 shows the evolution of the velocity along the tube. A wave pattern can

clearly be seen along the contour. These waves start with a low amplitude and continue

to increase. A snapshot of the velocity can be seen in Figure 2.2. The amplitude for each

wave can be seen increasing, with the lower frequencies dominating for the first portion

of the time interval. The wave then becomes irregular due to the third and fourth mode

gaining strength.

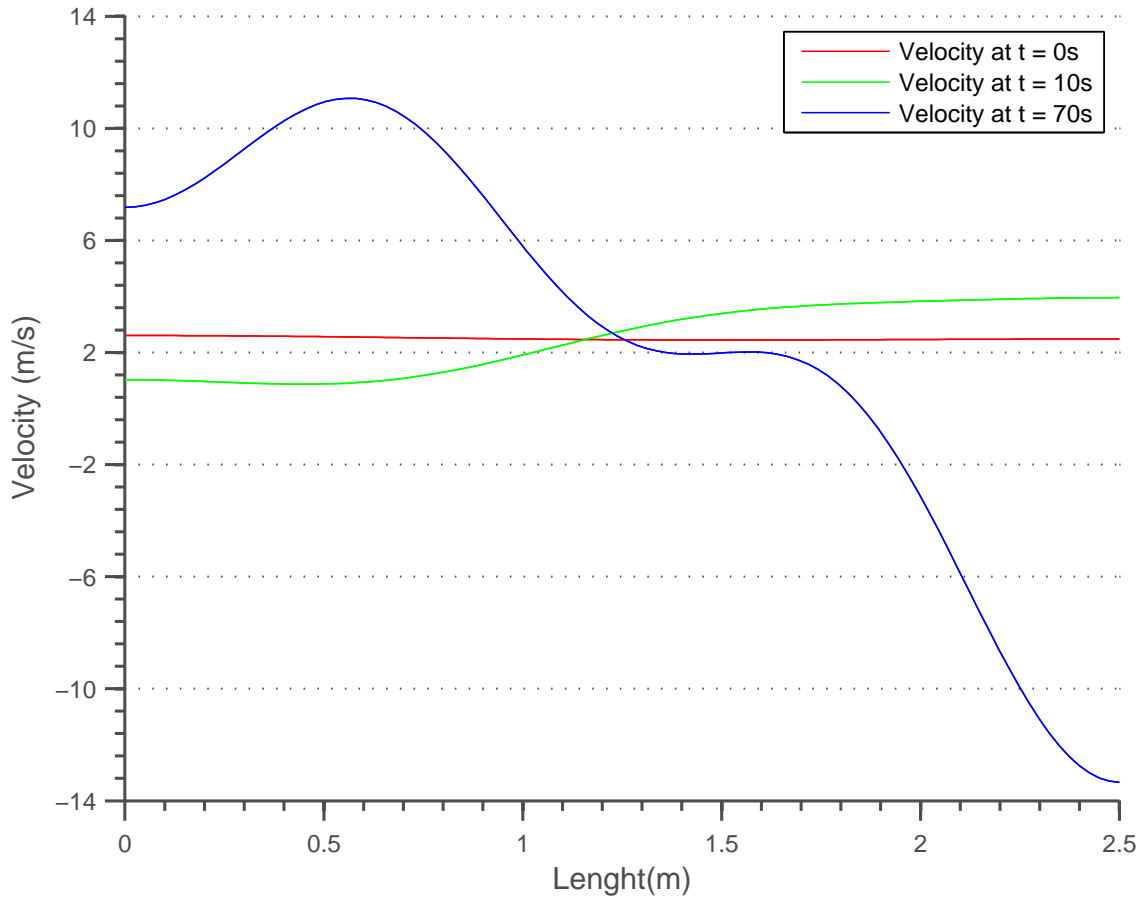The evolution of the aforementioned modes can be seen in Figures 2.3-2.4. Important

Figure 2.2: Time evolution of velocity along the Rijke tube.

facts about the development of the upper modes can be seen in said figures. The first two

modes start gaining a large amplitude within a small amount of time, the third natural mode

does so at around 10s, and the fourth at approximately 15s. This is due to our damping

parameter being large for the upper modes, something that our control scheme will exploit.

The evolution for the velocity and pressure disturbances at the heater location can be

seen in Figures 2.5-2.6. Due to the derivation of our approximate mathematical model,

we cannot obtain an accurate representation of a fully developed instability, due to the

higher frequencies carrying relevant information about the system. However, during the

transitional energy growth, which can be seen in Figure 2.7 between 0s and 20s, it can be
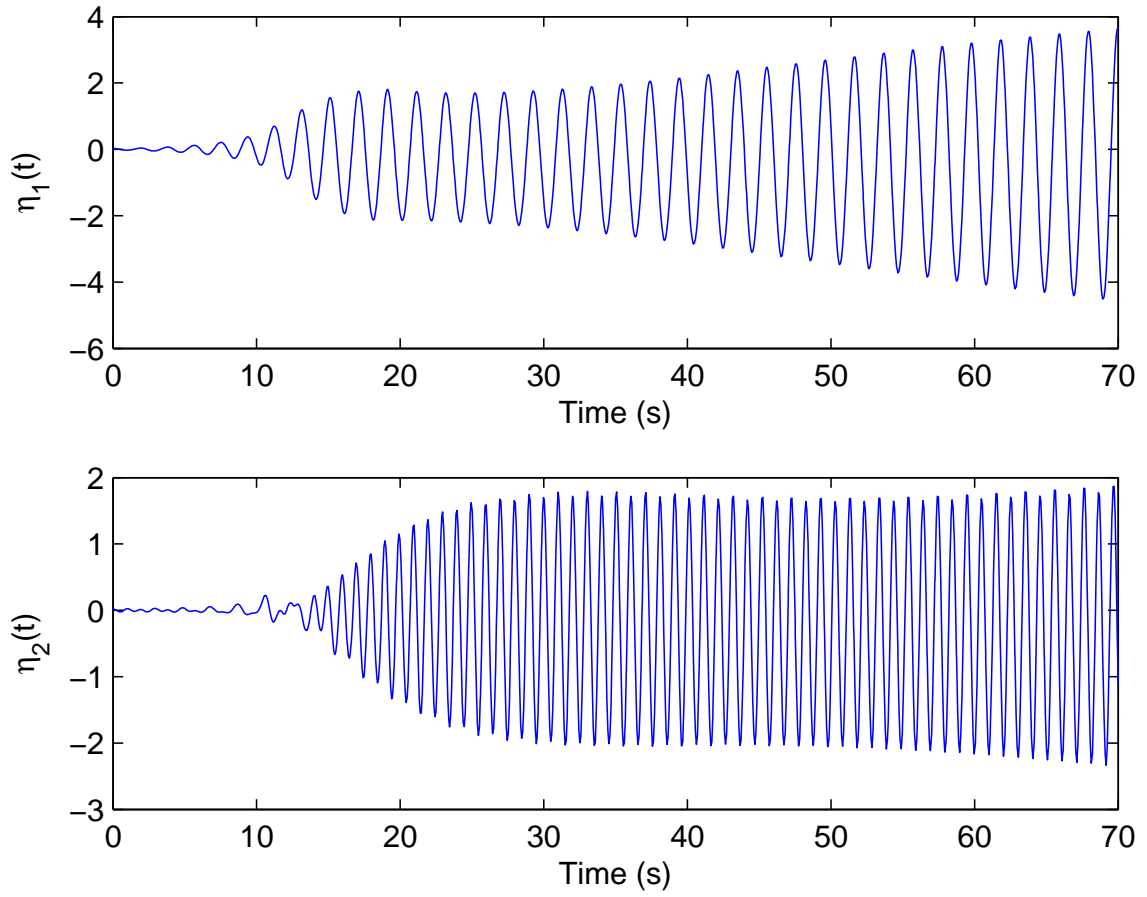
Figure 2.3: Nondimensional amplitude of the two lower modes.

seen that the lower frequencies are dominating in the pressure and velocity disturbances.

Similar results from this energy ratio can be found in [Zhao and Reyhanoglu (2014)].
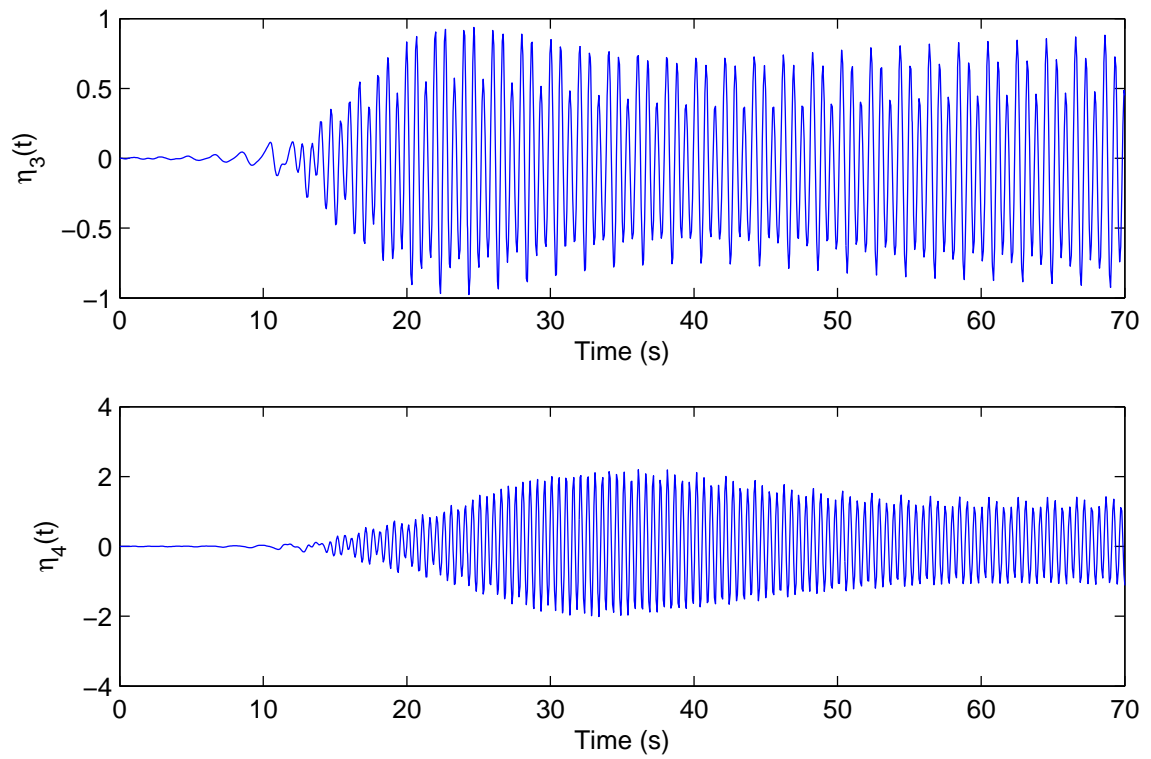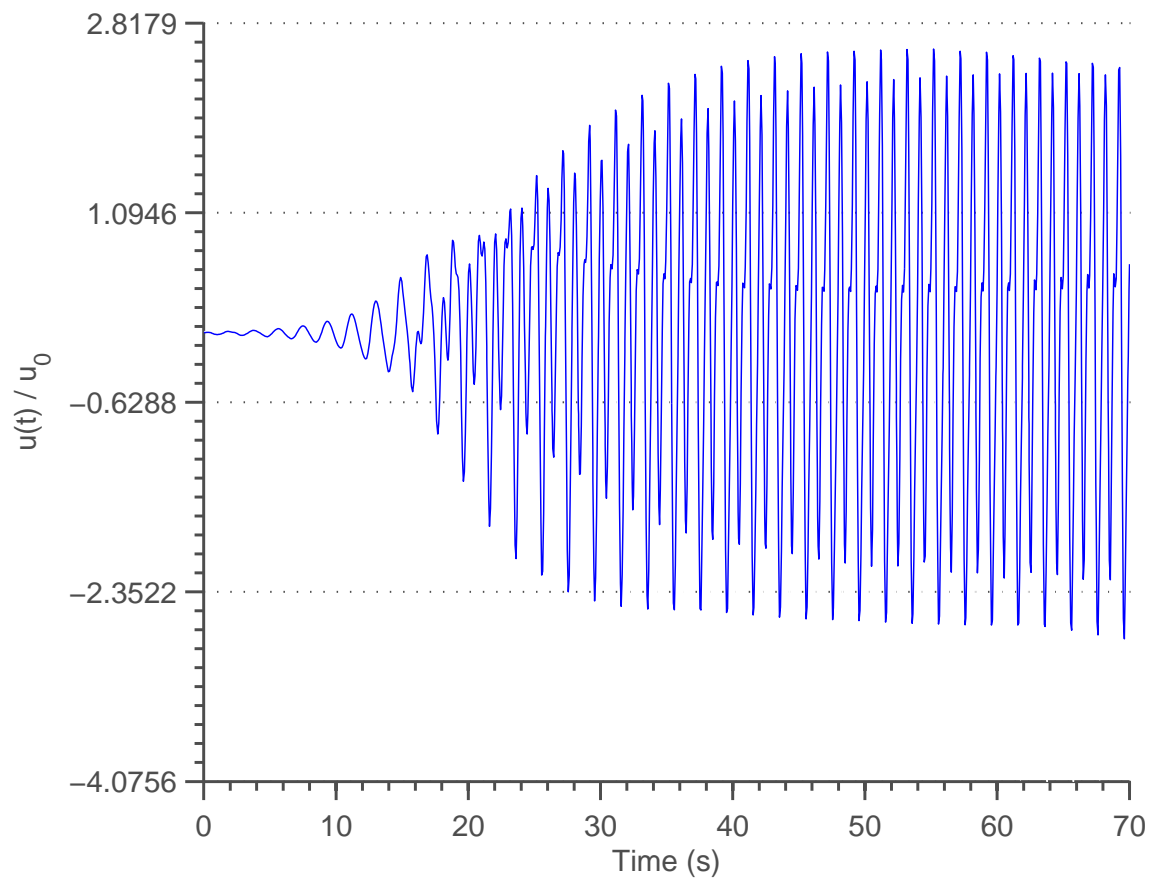
Figure 2.4: Upper modes of the system.

Figure 2.5: Evolution of velocity at one of the heaters' locations.
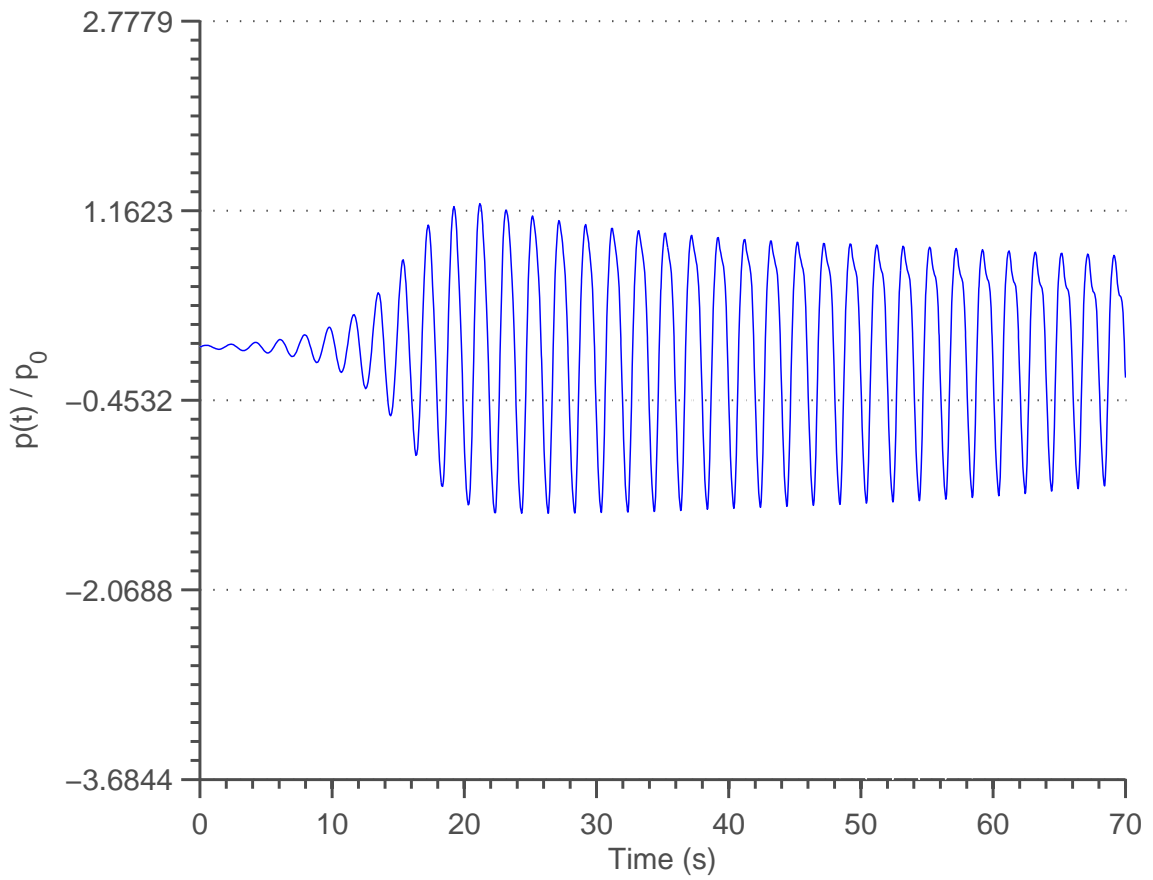
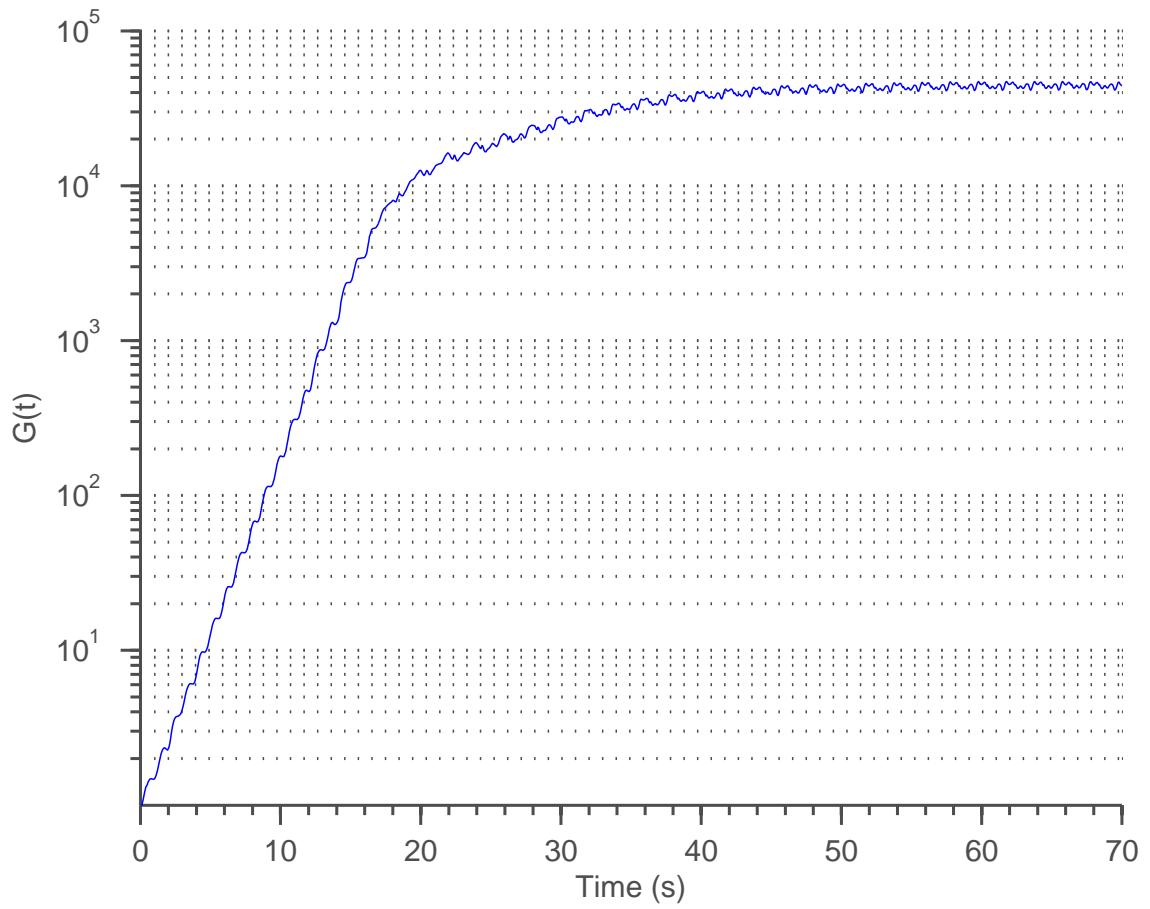Figure 2.6: Evolution of pressure at one of the heaters' location.

Figure 2.7: Evolution of the nondimensional energy ratio for an uncontrolled system.

Chapter 3

NONLINEAR FEEDBACK CONTROL

Following the formulation of equation (2.29) and its verification in Section 2.4, this chapter expands on the stability of said equation and explores different techniques to prevent the triggering of transient growth with a nonlinear controller and passive control.

Examples of linear controllers can be found in [Fleifil (2007)], [J. Rubio-Hervas (2015)], and [J. Rubio-Hervas (2014b)]. In one case the authors approach the problem with an Linear Quadratic Regulator (LQR). While the controller manages to minimize the linear portion, it fails to prevent the eventual transient growth. The trigger for such growth is due to the low-amplitude perturbations that can lead to a nonlinear cycle produced by the heat source. As such, nonlinear effects must be considered in the design of the controller.

3.1   Controller Design

In this section, a control algorithm is proposed for the system described in equation (2.29). Previous studies found in [Fleifil (2007)] create a linear expression from the nondimensional transformation of equation (2.17) to approximate the nonlinear portion, such that:

$$\dot{Q}_{sg} = \mathscr{K}_g \left[\sqrt{\left| \frac{1}{3} + u_{fg}(t - \tau_g) \right|} - \sqrt{\frac{1}{3}} \right] \approx \mathscr{K}_g \frac{\sqrt{3}}{2} u_{fg}(t - \tau_g) \tag{3.1}$$

Equation (4.1) is only valid only certain conditions, specifically if $\left| u_{fg}(t - \tau_g) \right| << 1$. The linearization will not be used in the controller development; however, will provide some insight on the eigenvalues of our ODE and some control design further studied in Section 4.1. Additional information can also be found in [Juniper (2013)].

To explore the capacity the actuators have to control the system, we write the actuator signal in terms of the Galerkin approximation. The heat release must also be written in this form. Equations (2.25) and (2.23) become:

$$v_{ak} = \mathscr{R}_k \sum_{i=1}^{N} \cos(i\pi x_{ak})\eta_i - \mathscr{S}_k \sum_{i=1}^{N} \frac{\sin(i\pi x_{ak})}{i\pi} \dot{\eta}_i(t) \tag{3.2}$$

Furthermore, combining equations (2.29) and (3.2) we can obtain the following system:

$$\ddot{\eta}_j + (j\pi)^2 \eta_j + \zeta_j \dot{\eta}_j = -2(\gamma - 1)j\pi \sum_{g=1}^{G} \dot{Q}_{sg}(x_{fg}, t - \tau_g) \sin(j\pi x_{fg})$$

$$-2\gamma j\pi \sum_{k=1}^{K} \alpha_{ak} \left[\mathscr{R}_k \sum_{i=1}^{N} \cos(i\pi x_{ak})\eta_i - \mathscr{S}_k \sum_{i=1}^{N} \frac{\sin(i\pi x_{ak})}{i\pi} \dot{\eta}_i(t) \right] \sin(j\pi x_{ak}) \tag{3.3}$$

This is the full representation of the thermoacoustic system with the nonlinear control pa-

rameters $\mathscr{R}_k$ and $\mathscr{S}_k$. Defining the following variables:

$$\dot{\hat{Q}}_{sgj} = -2(\gamma-1)j\pi\dot{Q}_{sg}(x_{fg},t-\tau_g)\sin(j\pi x_{fg}), \qquad \hat{R}_k = -2\gamma\pi\alpha_{ak}\mathscr{R}_k,$$

$$\hat{S}_k = 2\gamma\alpha_{ak}\mathscr{S}_k, \qquad A_{ijk} = \cos(i\pi x_{ak})\sin(j\pi x_{ak}), \qquad B_{ijk} = \frac{1}{i}\sin(i\pi x_{ak})\sin(j\pi x_{ak})$$

reduces equation (3.3) to:

$$\ddot{\eta}_j + (j\pi)^2\eta_j + \zeta_j\dot{\eta}_j = \sum_{g=1}^{G}\dot{\hat{Q}}_{sgj} + \sum_{k=1}^{K}\left(j\hat{R}_k\sum_{i=1}^{N}A_{ijk}\eta_i + j\hat{S}_k\sum_{i=1}^{N}B_{ijk}\dot{\eta}_i\right) \qquad (3.4)$$

Define the control input in terms of the control parameters:

$$j\hat{R}_k\sum_{i=1}^{N}A_{ijk}\eta_i + j\hat{S}_k\sum_{i=1}^{N}B_{ijk}\dot{\eta}_i = \beta_{jk}U_k \qquad (3.5)$$

This ensures that equation 3.4 may be further simplified as:

$$\ddot{\eta}_j + \zeta_j\dot{\eta}_j + (j\pi)^2\eta_j - \sum_{g=1}^{G}\dot{\hat{Q}}_{sgj} = \sum_{k=1}^{K}\beta_{jk}U_k \qquad (3.6)$$

Doing so allows the system to be expressed in matrix notation, such that all the superimposed modes are expressed with a single matrix equation.

$$
\begin{bmatrix}
\ddot{\eta}_1 + (\pi)^2 \eta_1 + \zeta_1 \dot{\eta}_1 - \sum_{g=1}^{G} \dot{\hat{Q}}_{sg1} \\[6pt]
\ddot{\eta}_2 + (2\pi)^2 \eta_2 + \zeta_2 \dot{\eta}_2 - \sum_{g=1}^{G} \dot{\hat{Q}}_{sg2} \\[6pt]
\vdots \\[6pt]
\ddot{\eta}_N + (N\pi)^2 \eta_n + \zeta_N \dot{\eta}_N - \sum_{g=1}^{G} \dot{\hat{Q}}_{sgN}
\end{bmatrix}
=
\begin{bmatrix}
\beta_{11} & \beta_{12} & \cdots & \beta_{1K} \\
\beta_{21} & \beta_{22} & \cdots & \beta_{2K} \\
\vdots & \vdots & \ddots & \vdots \\
\beta_{N1} & \beta_{N2} & \cdots & \beta_{NK}
\end{bmatrix}
\begin{bmatrix}
U_1 \\
U_2 \\
\vdots \\
U_K
\end{bmatrix}
\tag{3.7}
$$

The matrix β has K columns and N rows. β must also be invertible; to guarantee this we must make sure that: $det(\beta) \neq 0$, and the number of actuators must be equal or greater than the number of modes considered in the Galerkin approximation. For convenience, we will assume that β is squared ($K = N$).

We will design a nonlinear control law such that the closed loop system takes the following form:

$$
\ddot{\eta}_j + k_{j2} \dot{\eta}_j + k_{j1} \eta_j = 0
\tag{3.8}
$$

with the respective values k_{j2} and k_{j1} so that the solution is not an exponential increase. Recall that the solution for equation (3.8) can be written as:

$$
\eta_j = A_j e^{-\frac{k_{j2} + \sqrt{k_{j2}^2 - 4k_{j1}}}{2}} + B_j e^{-\frac{k_{j2} - \sqrt{k_{j2}^2 - 4k_{j1}}}{2}}
\tag{3.9}
$$

It can be seen with equation (3.9) that to achieve exponential decay, the condition $k_{j2} > \sqrt{k_{j2}^2 - 4k_{j1}}$ has to be met. Additionally, to prevent any oscillations, $Im\left(\sqrt{k_{j2}^2 - 4k_{j1}}\right) =$

0. The correct values for k_{j2} and k_{j1} must be chosen such that they meet said conditions. These conditions can be satisfied by setting $k_{j2} > 0$ and $\frac{k_{j2}^2}{4} > k_{j1} > 0$. The solution for the control vector U can be written as:

$$
\begin{bmatrix} U_1 \\ U_2 \\ \vdots \\ U_N \end{bmatrix} = \begin{bmatrix} \beta_{11} & \beta_{12} & \cdots & \beta_{1N} \\ \beta_{21} & \beta_{22} & \cdots & \beta_{2N} \\ \vdots & \vdots & \ddots & \vdots \\ \beta_{N1} & \beta_{N2} & \cdots & \beta_{NN} \end{bmatrix}^{-1}
$$
$$
\times \begin{bmatrix} ((\pi)^2 - k_{12})\eta_1 + (\zeta_1 - k_{11})\dot{\eta}_1 - \sum_{g=1}^{G} \dot{\hat{Q}}_{sg1} \\ ((2\pi)^2 - k_{22})\eta_2 + (\zeta_2 - k_{21})\dot{\eta}_2 - \sum_{g=1}^{G} \dot{\hat{Q}}_{sg2} \\ \vdots \\ ((N\pi)^2 - k_{N2})\eta_N + (\zeta_N - k_{N1})\dot{\eta}_N - \sum_{g=1}^{G} \dot{\hat{Q}}_{sgN} \end{bmatrix}
$$

(3.10)

We now need to build the β matrix and assign a value to U_k based on the actuation signal. Choose:

$$
\beta_{1k} = 1 \qquad \forall k \tag{3.11}
$$

and

$$
A_{i1k} = j\phi_{jk}A_{ijk} \qquad \forall i, j, k, j \neq 1 \tag{3.12}
$$

which implies

$$
B_{i1k} = j\phi_{jk}B_{ijk} \qquad \forall i, j, k, j \neq 1 \tag{3.13}
$$

The control transformation in equation (3.6) would then become:

$$\hat{R}_k \sum_{i=1}^{N} A_{i1k}\eta_i + \hat{S}_k \sum_{i=1}^{N} B_{i1k}\dot{\eta}_i = U_k \qquad \forall k \tag{3.14}$$

where ϕ_{jk} is a parameter dependent on the location of the *kth* actuator. The matrix β can then be written as:

$$\beta = \begin{bmatrix} 1 & 1 & \cdots & 1 \\ \frac{1}{\phi_{21}} & \frac{1}{\phi_{22}} & \cdots & \frac{1}{\phi_{2N}} \\ \vdots & \vdots & \ddots & \vdots \\ \frac{1}{\phi_{N1}} & \frac{1}{\phi_{N2}} & \cdots & \frac{1}{\phi_{NN}} \end{bmatrix} \tag{3.15}$$

The control parameters can then be recovered through the following equations:

$$\hat{R}_k = \frac{\sum_{i=1}^{N} A_{i1k}\eta_i}{\left(\sum_{i=1}^{N} A_{i1k}\eta_i\right)^2 + \left(\sum_{i=1}^{N} B_{i1k}\dot{\eta}_i\right)^2} U_k \tag{3.16}$$

$$\hat{S}_k = \frac{\sum_{i=1}^{N} B_{i1k}\dot{\eta}_i}{\left(\sum_{i=1}^{N} A_{i1k}\eta_i\right)^2 + \left(\sum_{i=1}^{N} B_{i1k}\dot{\eta}_i\right)^2} U_k \tag{3.17}$$

Using the value for U_k obtained through the matrix equation (3.10) allows to calculate the control parameters for each actuator. These will change over time and eventually converge to a final value.

3.1.1 Actuator Location

The value of the elements of the β matrix affects the control input U_k which also affects the control parameters $\mathscr{R}_k$ and $\mathscr{S}_k$. The values in the matrix can then be tuned by changing the location of the actuators.

From the relations in equations (3.12)-(3.13), the value of ϕ_{jk} can be obtained with the following equation:

$$\phi_{jk} = \frac{1}{j^2 \cos(x_{ak}\pi)} \tag{3.18}$$

Due to the conditions imposed on the β matrix, the position of the actuators is restricted. Actuator locations should be chosen such that the system is controllable.

3.2 Testing the Performance of the Controller

This section is dedicated to test the performance of the controller under a specific scenario. The control parameters are used to see if the actuators can perform the necessary tasks while using a reasonable magnitude of the actuation signal.

For the initial conditions, only the velocity is assumed to have a disturbance, with a low frequency wave. For the initial conditions, only the velocity is assumed to have a disturbance, with a low frequency wave. The same parameters found in Table 2.1 are used in the performance test with the addition of the actuators at locations x_{f1} and x_{f2}.

Table 3.1: List of parameters for performance testing.

List of Parameters			
Parameter	Value	Parameter	Value
ρ	$1.025\frac{\text{kg}}{\text{m}^3}$	λ	$0.0328\frac{\text{m}^2}{\text{s}}$
c_v	$719\frac{\text{J}}{\text{kgK}}$	γ	0.4
L_0	1m	T_b	295K
c	$344.64\frac{\text{m}}{\text{s}}$	u_0	$2.5\frac{\text{m}}{\text{s}}$
L_w	2.5m		
d_{w1}	$0.5\times 10^{-3}\text{m}$	d_{w2}	$0.5\times 10^{-3}\text{m}$
T_{w1}	1800K	T_{w2}	1800K
x_{f1}	0.625m	x_{f2}	1m
x_{a1}	0.98m	x_{a2}	1.52m
τ_1	1000ms	τ_2	500ms
P_0	$8.69\times 10^4\text{Pa}$	S_c	$1.56\times 10^{-3}\text{m}^2$
c_1	0.04	c_2	0.004

3.2.1   Controller with Two Actuators

For this test case, the controller is assumed to have two actuators at its disposal. Due to our conditions for our β matrix, only the two lower modes will be able to be controlled. In Figure 3.1 we can see the evolution of velocity along the length of the tube. As it can be seen, it successfully stabilizes to $u = 2.5\frac{\text{m}}{\text{s}}$, which is the value of the mean flow of the fluid. This can be seen better in Figure 3.2.

In figure 3.3, the combined acoustic energy of the disturbances in the two lower modes successfully converges to zero. The system does not experience any triggering as $G(t) < 1$ at all times.

The value of the control parameters for each actuator can be seen in Figures (3.4)-(3.5). The value of these parameters converge to a constant, despite the fact that our control U_k is dependent on the product between the velocity disturbance and $\mathscr{R}_k$, and the pressure disturbance and $\mathscr{S}_k$. This indicates that our control input will also converge to zero.
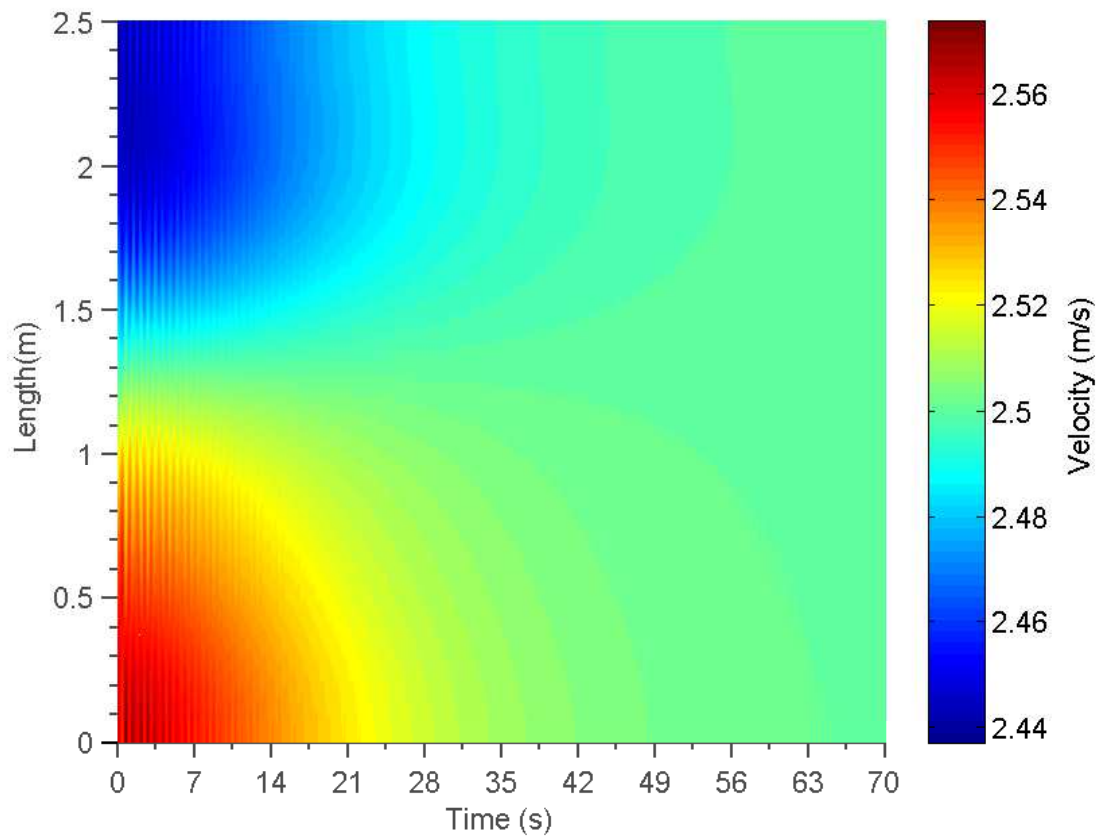
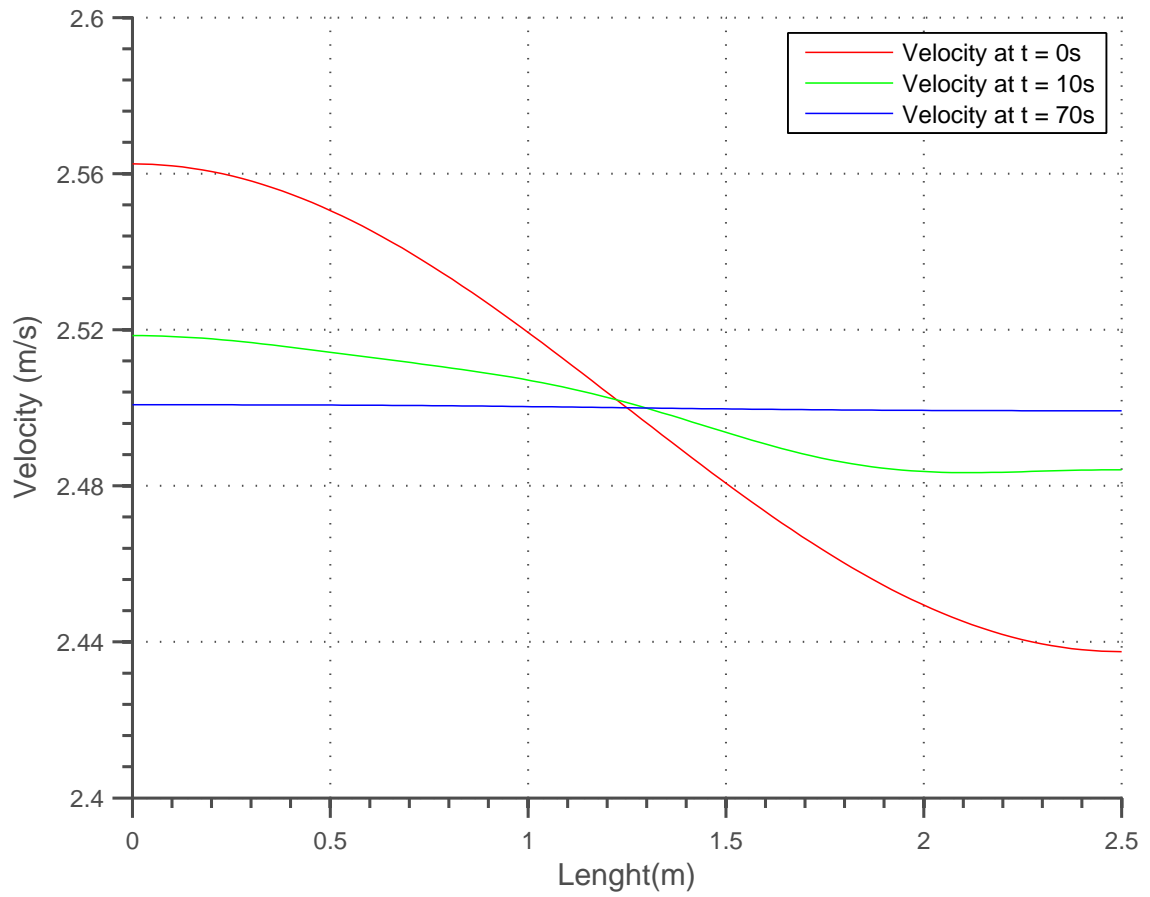Figure 3.1: Contour plot of fully controlled system.

Figure 3.2: Snapshot of velocity at time $t = 0s$, $t = 10s$ and $t = 70s$.
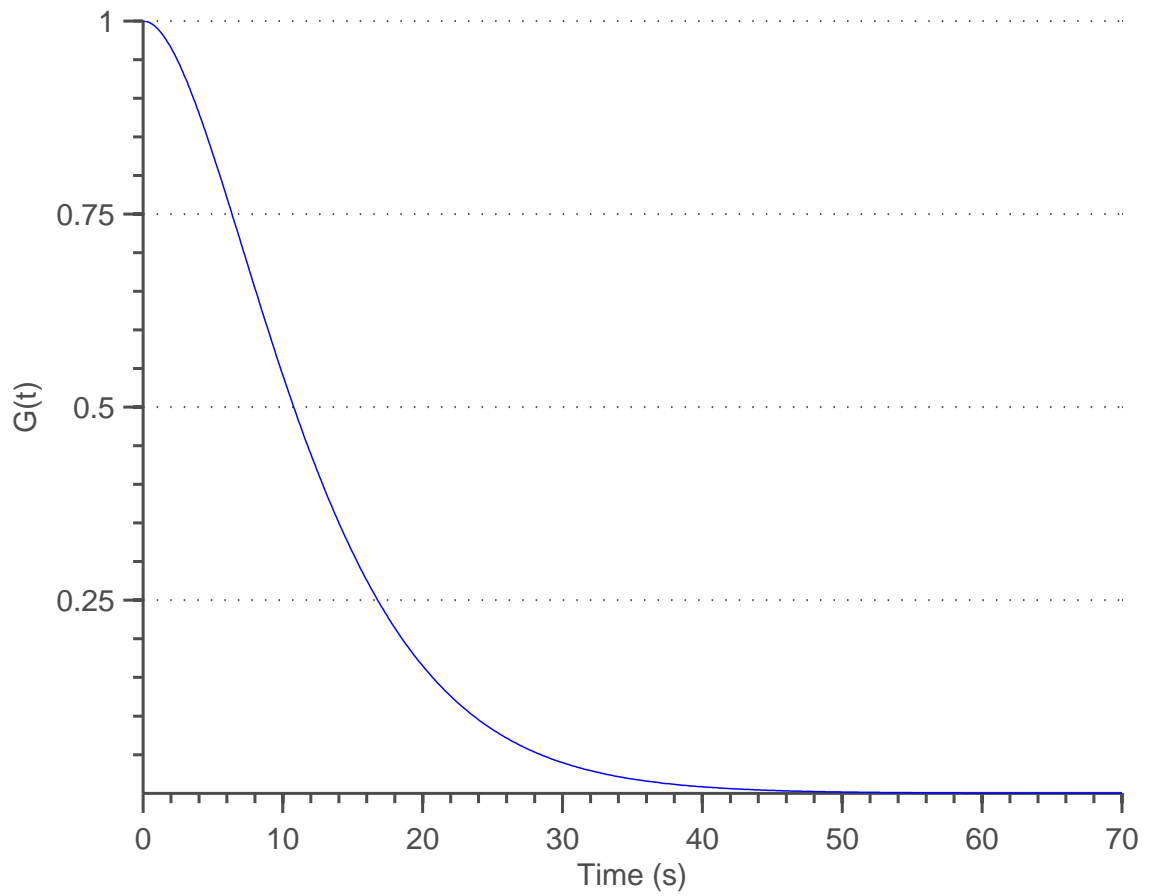
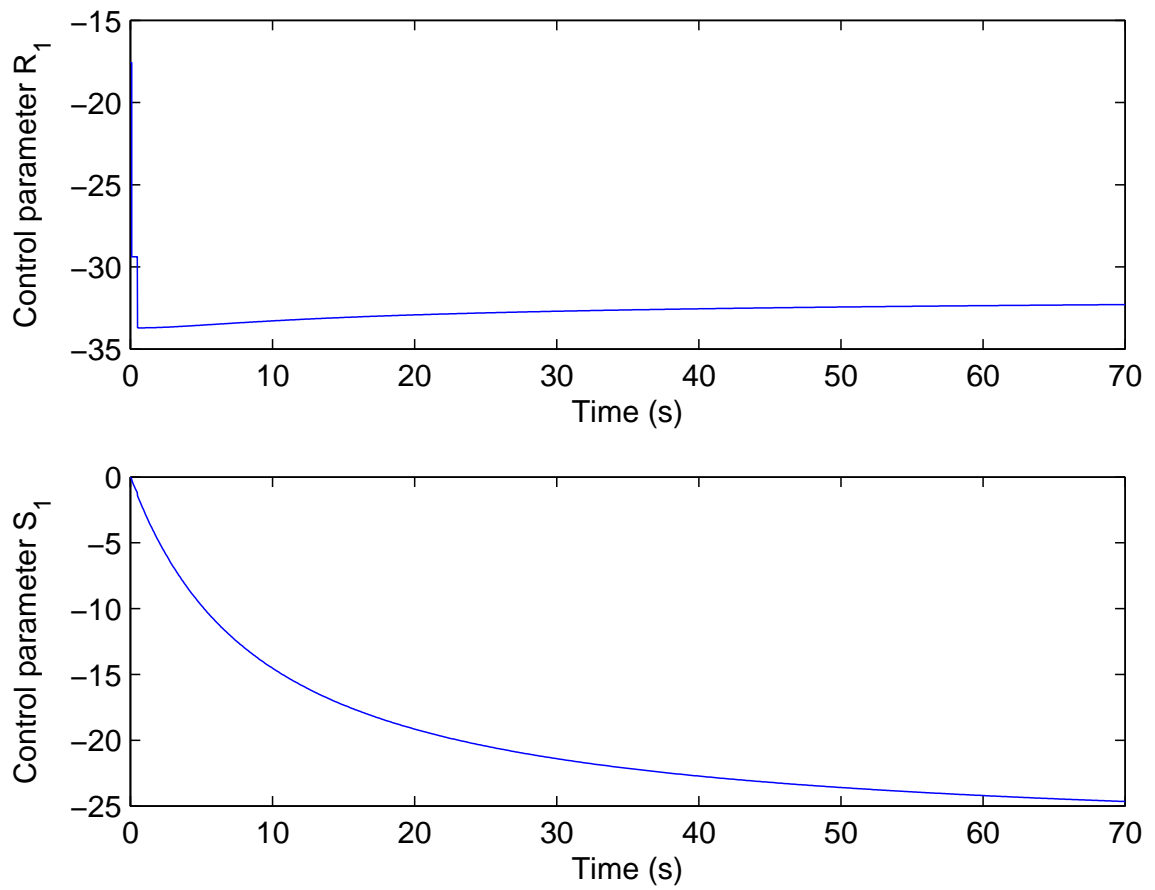Figure 3.3: Acoustic energy of the low frequency waves.

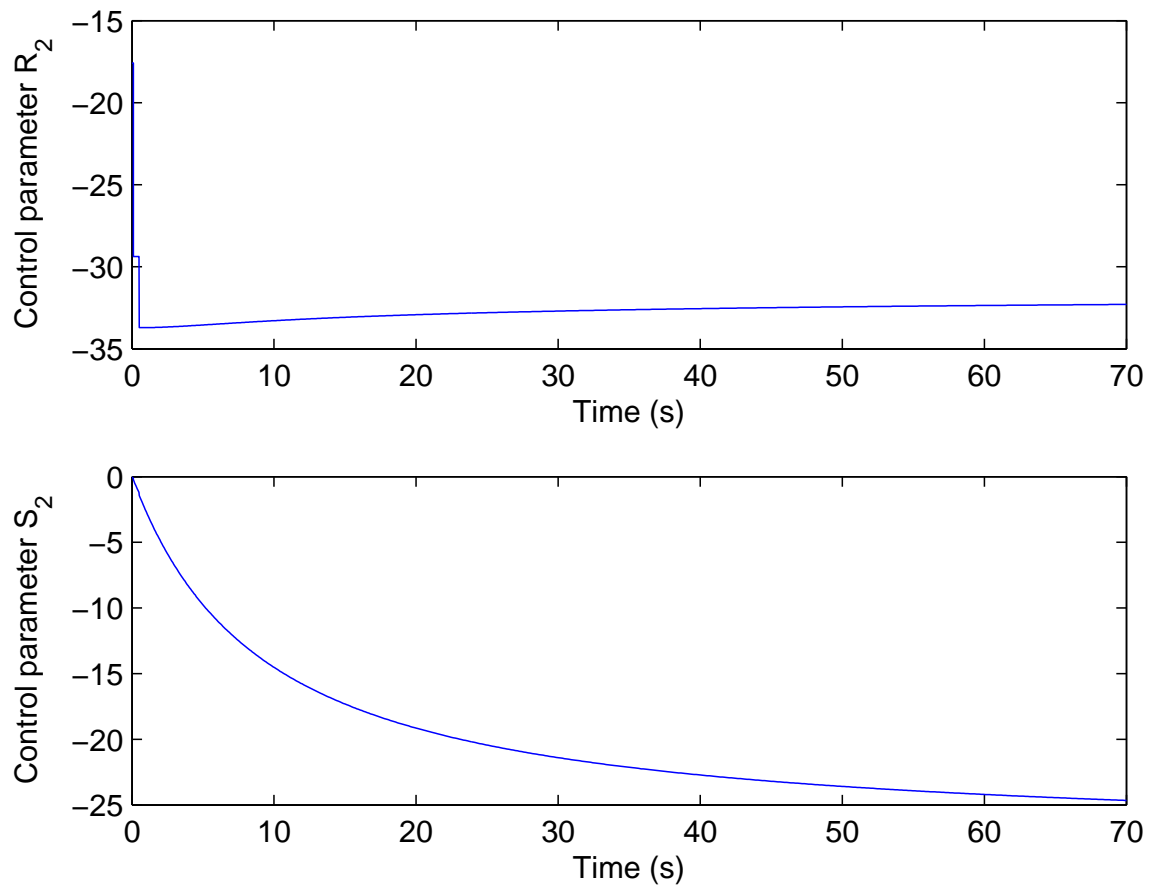Figure 3.4: Control parameters for actuator 1.

Figure 3.5: Control parameters for actuator 2.

3.2.2 Effect on Higher Frequency Modes

The heat release is highly dependent on disturbances on the velocity. If these are present in the higher frequencies, it could indirectly affect the converging value of the control parameters.

With Figure 3.6 we see an a small initial growth, coming from the higher modes. This is the transient growth being triggered by the thermoacoustic instability in the high frequency modes. The controller cannot prevent this directly, but it is able to dissipate the energy being transfered to the lower frequency waves, eventually stabilizing the system. The behavior for the amplitude of the waves can be seen in Figures 3.7 and 3.8.
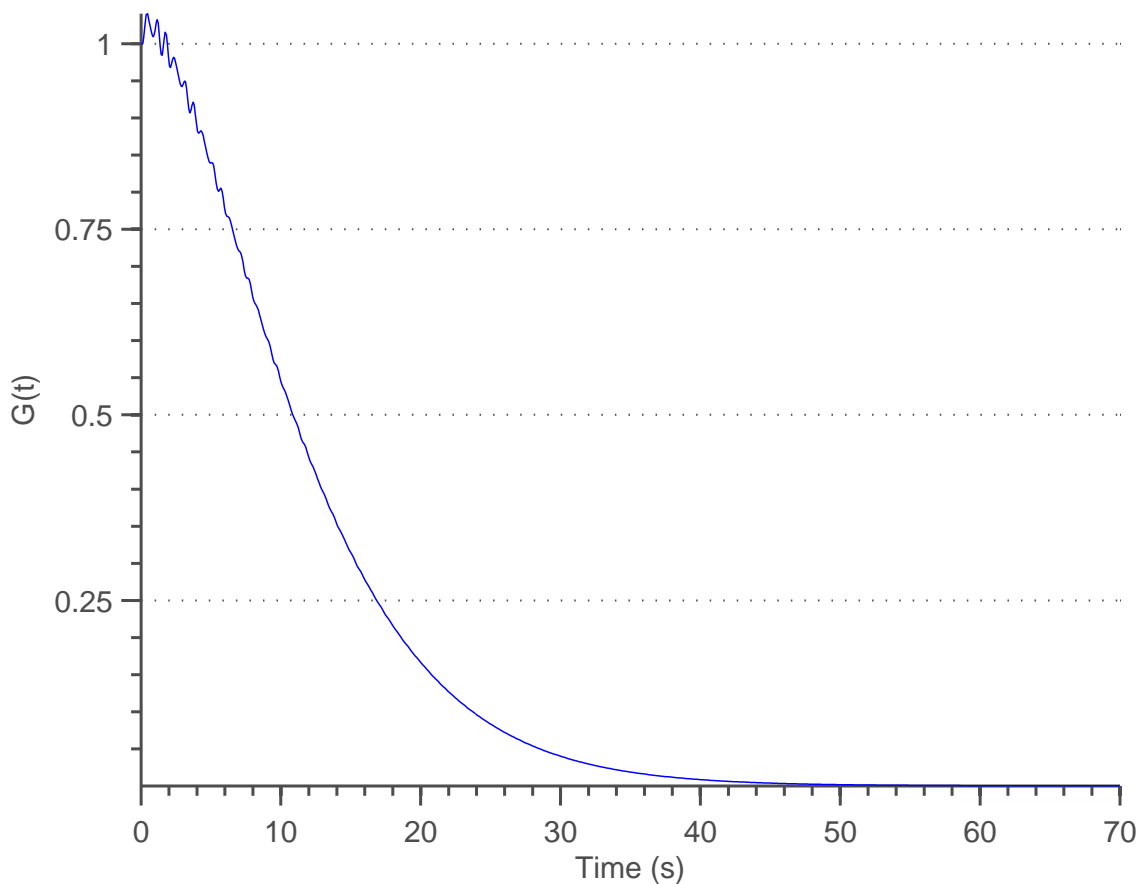

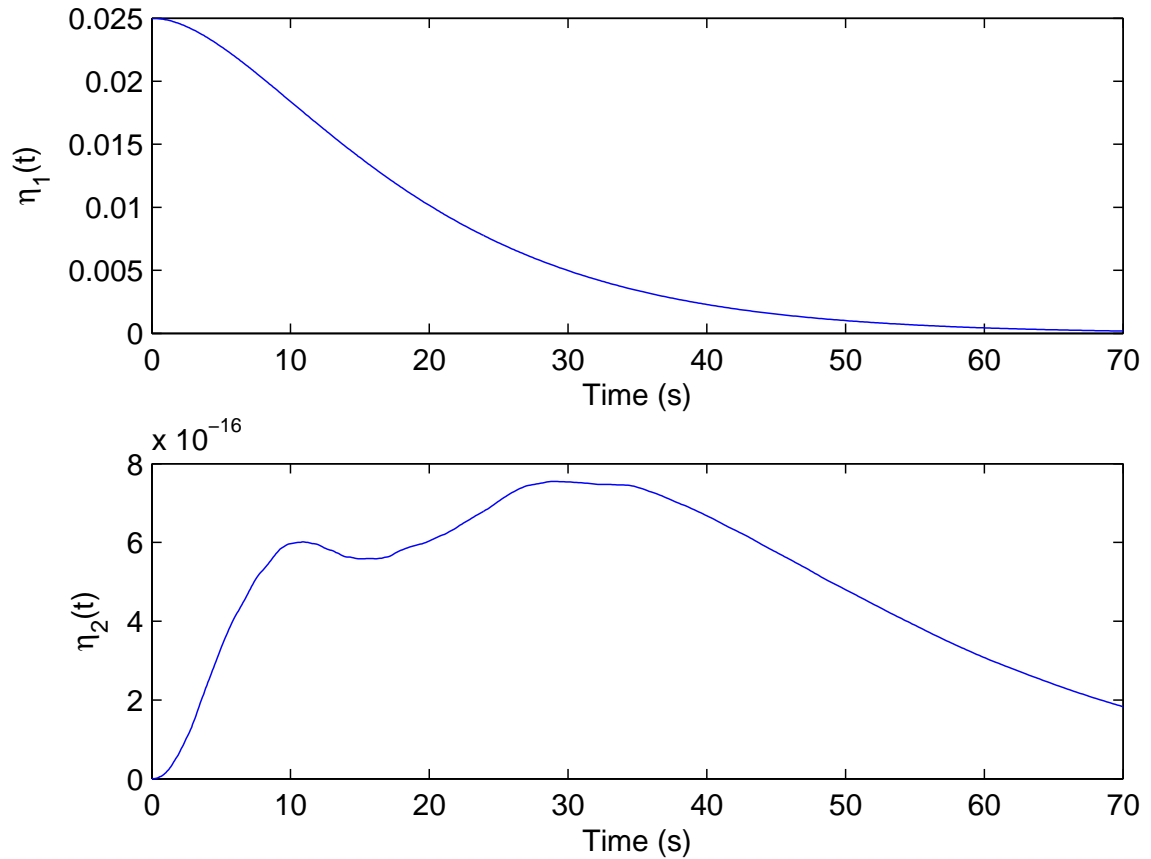Figure 3.6: Acoustic energy of the system.

Figure 3.7: Evolution of the amplitude of low frequency modes.

Following, the evolution of the velocity and pressure disturbances can be seen under Figures 3.9 and 3.10. One of the most striking factors is the presence of jitter in the velocity disturbance. This correlates to the "unstable" period the that can be seen in the uncontrolled modes in Figure 3.8. The pressure disturbance experiences a similar behavior, though it is less apparent due to the derivative initial conditions being set to zero.
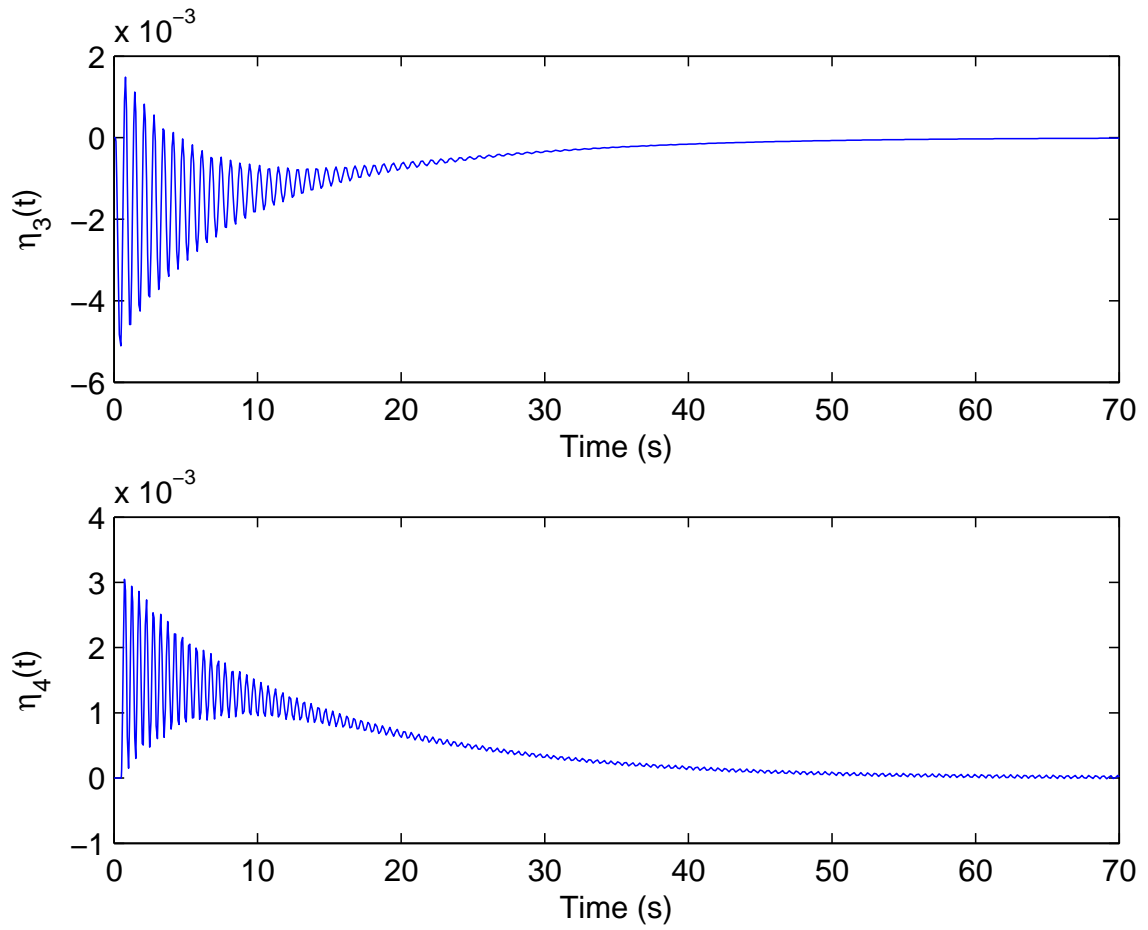
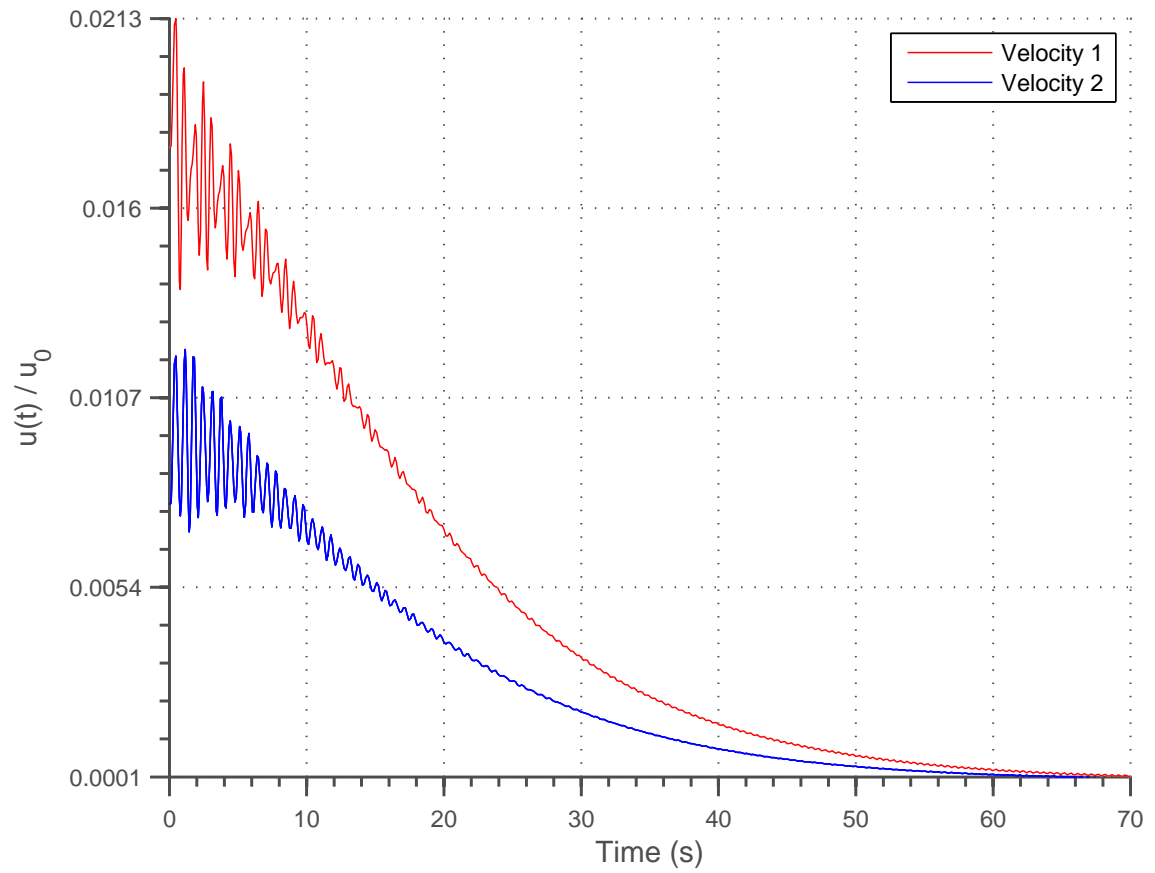Figure 3.8: Evolution of the amplitude of high frequency modes.

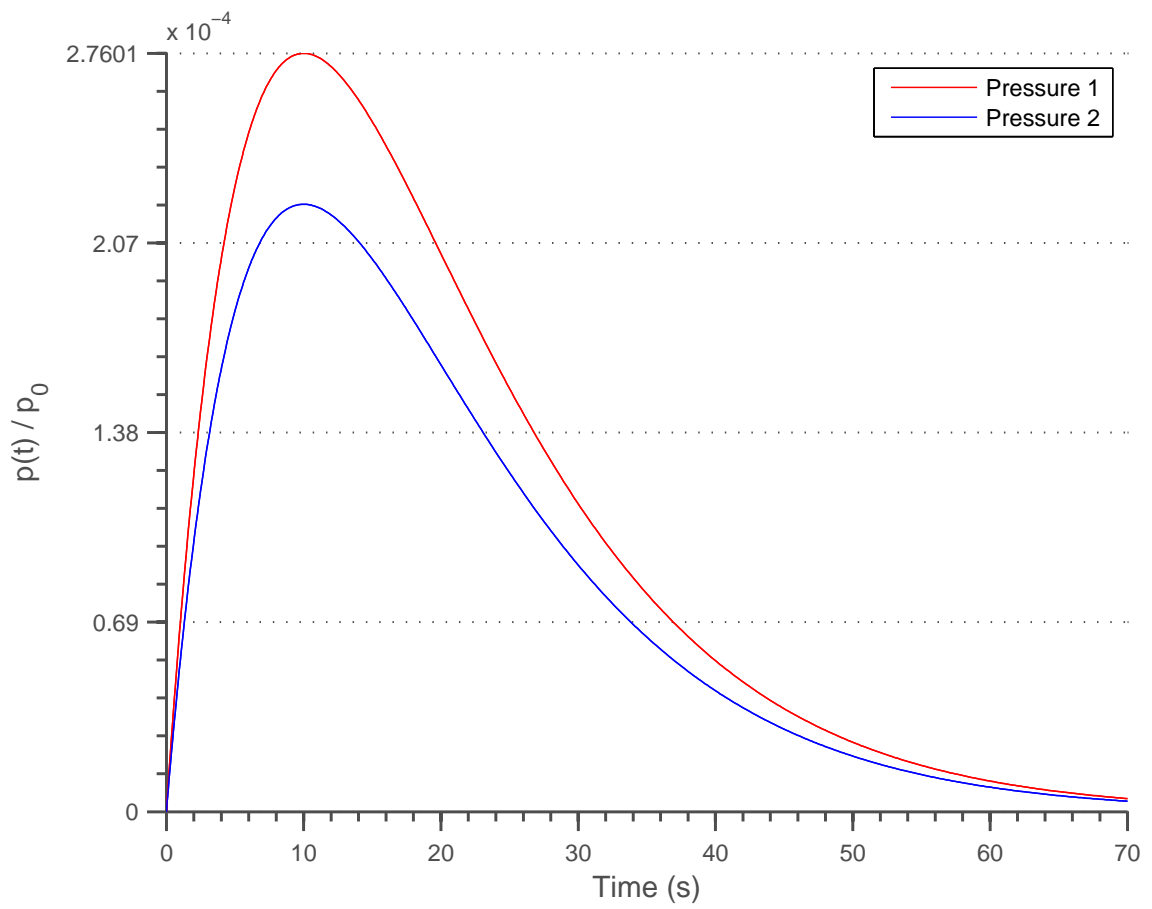Figure 3.9: Velocity for heat source 1 and 2 (x_{f1} and x_{f2} respectively)

Figure 3.10: Pressure for heat source 1 and 2 (x_{f1} and x_{f2} respectively)

Chapter 4

EFFECT OF MULTIPLE HEAT

SOURCES

4.1   Passive Control with Multiple Heat Sources

There are several factors that can affect the "cost" of the control parameters. Positioning

of the heat sources is known to affect the heat release and the rate at which the instabilities

grow. There have been models that have shown to stabilize the system by the addition of a

careful placed second heater [Ji (2014)]. However, the presence of this "passive" controller

does not eliminate the disturbances in the system; it simply prevents the triggering of the

transient growth. By using equation (3.1) we linearize the heat release shown as:

$$\dot{Q}_{sg} \approx \mathscr{K}_g \frac{\sqrt{3}}{2} \sum_{j=1}^{N} \cos(j\pi x_{fg}) \eta_j (t - \tau_g) \qquad (4.1)$$

By substituting into equation (3.3), we can obtain a linearized system described by the

following ODE:

$$\ddot{\eta}_j + (j\pi)^2\eta_j + \zeta_j\dot{\eta}_j = -2(\gamma-1)j\pi \sum_{g=1}^{G} \sin(j\pi x_{fg})\mathscr{K}_g \frac{\sqrt{3}}{2} \sum_{j=1}^{N} \cos(j\pi x_{fg})\eta_j(t-\tau_g)$$

$$-2\gamma j\pi \sum_{k=1}^{K} \alpha_{ak} \left[\mathscr{R}_k \sum_{i=1}^{N} \cos(i\pi x_{ak})\eta_i + \mathscr{S}_k \sum_{i=1}^{N} \frac{\sin(i\pi x_{ak})}{i\pi}\dot{\eta}_i(t) \right] \sin(j\pi x_{ak})$$

$$(4.2)$$

For convenience, let us assume that there is one predominant mode, no time delay τ_g, and no actuators are acting on the system. It was shown in equation (2.4) that any instability in the upper modes is dependent on the growth of the lower modes, therefore we can assume that any triggering in the low frequency range will be transmitted to the high frequency components. The following is the simplified equation:

$$\ddot{\eta}_1 + \pi^2\eta_1 + \zeta_1\dot{\eta}_1 = -(\gamma-1)\pi \sum_{g=1}^{G} \mathscr{K}_g\sqrt{3}\sin(\pi x_{fg})\cos(\pi x_{fg})\eta_1(t-\tau_g)$$

As it can be seen, it is a simple second order ODE. It can be rearranged to obtain the following:

$$\ddot{\eta}_1 + \underbrace{\zeta_1}_{b}\dot{\eta}_1 + \underbrace{\left(\pi^2 + (\gamma-1)\pi \sum_{g=1}^{G} \mathscr{K}_g\sqrt{3}\sin(\pi x_{fg})\cos(\pi x_{fg}) \right)}_{c}\eta_1 = 0 \qquad (4.3)$$

A solution for this type of equation can be found in Section 3 with equations (3.8)-(3.9). In order for the system to be exponentially stable, the eigenvalues, λ_1 and λ_2, must be positive

and real. As such they have to meet the following conditions:

$$-\frac{b \pm \sqrt{b^2 - 4c}}{2} \leq 0$$

$$b^2 - 4c \geq 0$$

which imply the following

$$c \leq \frac{b^2}{2}$$

for negative eigenvalues and

$$c \leq \frac{b^2}{4}$$

for real eigenvalues.

Let us now assume that we can control the positioning of heat sources $g = 1$ such that it is our "passive" controller. For an equation with the form of (4.3), it is know that the following condition will make it exponentially stable.

$$\pi^2 + (\gamma - 1)\pi\sqrt{3}\left(\mathcal{K}_1 \sin(\pi x_{f1})\cos(\pi x_{f1}) + \sum_{g=2}^{G} \mathcal{K}_g \sin(\pi x_{fg})\cos(\pi x_{fg})\right) \leq \frac{\zeta_1^2}{4} \quad (4.4)$$

This results in a domain solution for x_{f1} given as:

$$\frac{-\sin^{-1}\left(\frac{\zeta_1^2 - 4\pi^2 - 4(\gamma-1)\pi\sqrt{3}\sum_{g=2}^{G} \mathcal{K}_g \sin(\pi x_{fg})\cos(\pi x_{fg})}{(\gamma-1)2\pi\sqrt{3}\mathcal{K}_1}\right) + 2\pi n - \pi}{2\pi} \leq x_{f1} \leq$$

$$\frac{\sin^{-1}\left(\frac{\zeta_1^2 - 4\pi^2 - 4(\gamma-1)\pi\sqrt{3}\sum_{g=2}^{G} \mathcal{K}_g \sin(\pi x_{fg})\cos(\pi x_{fg})}{(\gamma-1)2\pi\sqrt{3}\mathcal{K}_1}\right) + 2\pi n}{2\pi} \quad (4.5)$$

Where $\zeta_1 \geq 0$; and $\mathcal{K}_1 > \frac{\zeta_1^2 - 4\pi^2 - 4(\gamma-1)\pi\sqrt{3}\sum_{g=2}^{G}\mathcal{K}_g\sin(\pi x_{fg})\cos(\pi x_{fg})}{2\pi\sqrt{3}(\gamma-1)}$. The acoustic length of

the system is 1. $n = 0$ would give a trivial solution for x_{f1} and $n = 2$ would take the upper

limit outside of our acoustic length; therefore, $n = 1$.

An interesting note is that trivializing the problem (No damping on the system and no

additional heat sources) for $n = 1$ gives the following solution for the flame location

$$\frac{1}{2} \leq x_{f1} \leq 1$$

Recall that 1 is the acoustic length of the system. This indicates that any position

between the upper half of the tube will cause a decay of any perturbation and will not allow

for any instabilities. This was observed experimentally by Rijke, and was found in his

earliest notes regarding this phenomenon.

Additionally, equation (4.5) gives as a condition a minimum value for $\mathcal{K}_1$ which indi-

cates two things. First of all, $\mathcal{K}_1$ may be negative or positive, which means that a heat sink

or a heat source can be used, while affecting the domain for x_{f1}. Second of all, there is no

maximum value for $\mathcal{K}_1$, which means the flame can be set at any temperature above the

mean temperature of the fluid. Note that increasing this, will drastically reduce the domain

of the system. Nevertheless, combustion system cannot afford to put heat sinks inside their

chambers without reducing their overall efficiency, an additional heat source is more viable.

4.1.1 Effect of Heater Location

In order to test our initial hypothesis we can offer a simplified case for equation (4.5). Any damping in the system will simply increase the domain where for our control flame location; so we can set it to zero. Additionally, we can simply describe a system with two heaters, the first one ($g = 1$) we can set the position and flame temperature. The second one ($g = 2$) is uncontrolled. The heat coefficients are such that $\mathscr{K}_1 = \mathscr{K}_2$. This gives that our domain given by:

$$\frac{-\sin^{-1}\left(-2\sin(\pi x_{f2})\cos(\pi x_{f2})\right) + 2\pi n - \pi}{2\pi} \leq x_{f1} \leq$$
$$\frac{\sin^{-1}\left(-2\sin(\pi x_{f2})\cos(\pi x_{f2})\right) + 2\pi n}{2\pi}$$

Which can be further simplified:

$$\frac{\sin(2\pi x_{f2}) + 2\pi n - \pi}{2\pi} \leq x_{f1} \leq \frac{-\sin(2\pi x_{f2}) + 2\pi n}{2\pi} \tag{4.6}$$

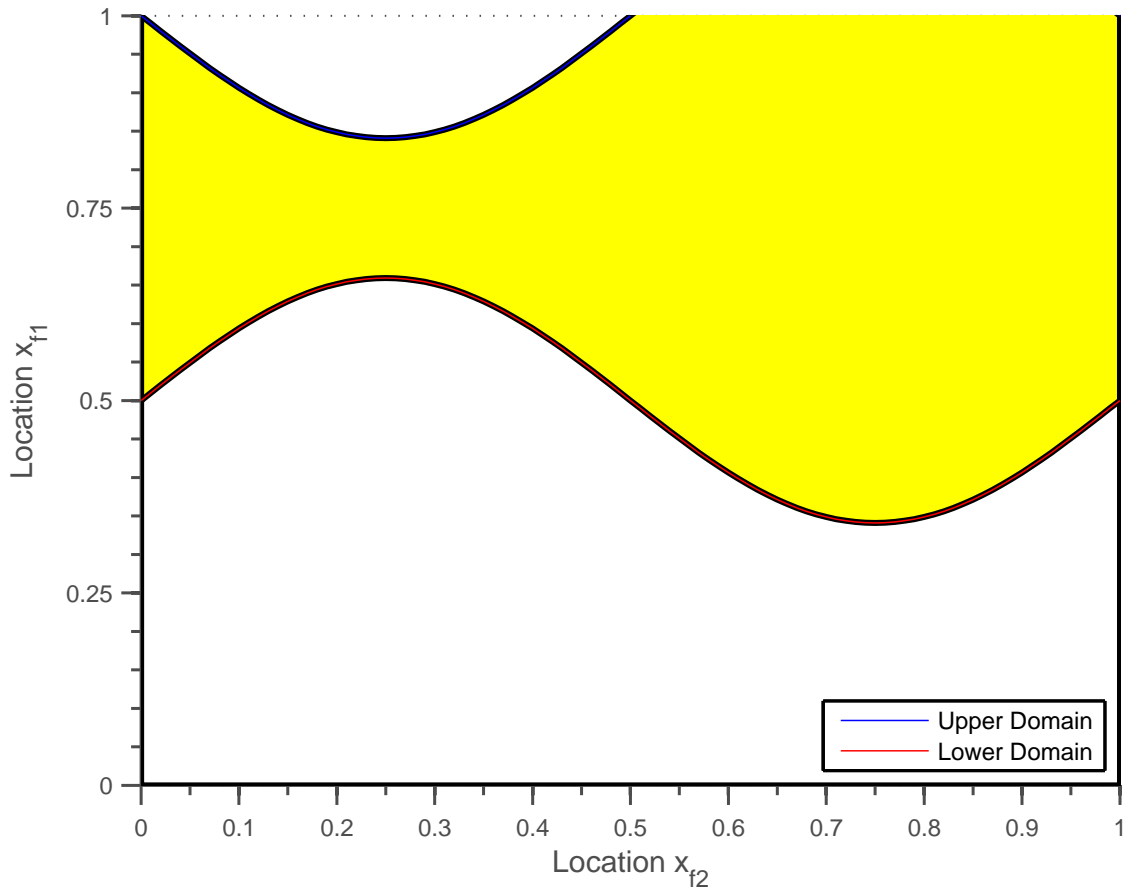A graphical representation of the domain can be found in Figure 4.1:

Figure 4.1: Graphs representation of domain for equation (4.6).

Note that this is only for the linear portion of the heat release. Placing the controlled heater inside the domain, will cause system to be stable, provided that any nonlinearity is not dominating. After a long time, it is expected that the system will become unstable in one of the modes. Following is a simulation of a system without actuators, and two heat sources. One of these sources has been placed inside the domain described in Figure 4.1.

Table 4.1: Parameters used for testing passive control.

List of Parameters			
Parameter	Value	Parameter	Value
ρ	$1.025\frac{kg}{m^3}$	λ	$0.0328\frac{m^2}{s}$
c_v	$719\frac{J}{kgK}$	γ	0.4
L_0	$1m$	T_b	$295K$
c	$344.64\frac{m}{s}$	u_0	$2.5\frac{m}{s}$
L_w	$2.5m$		
d_{w1}	$0.5 \times 10^{-3}m$	d_{w2}	$0.5 \times 10^{-3}m$
T_{w1}	$1800K$	T_{w2}	$1800K$
x_{f1}	$1.875m$	x_{f2}	$0.625m$
τ_1	$500ms$	τ_2	$100ms$
P_0	$8.69 \times 10^4 Pa$	S_c	$1.56 \times 10^{-3}m^2$
c_1	0.04	c_2	0.004

The evolution of the modes can be seen in Figures (4.2)-(4.3). It is not exactly an exponential decay as there are obvious oscillations for all of the modes. Despite the approximation, the second heater is able to reduce the modes to a value close to zero. It is worth nothing that the 4th mode experiences a growth after some time, and begin to oscillate between 10^{-6} and -10^{-6}. The low value of the amplitude, makes the growth of little concern. However, due to the nature of the duct, any kind of small disturbance could provoke an unstable growth of energy. Nevertheless, in figure 4.4, a clear decay can be seen. The initial growth is due to the delay of the second heat source; after which the system stabilizes. The development of the velocity and pressure disturbances can be found in Figures 4.5-4.6.
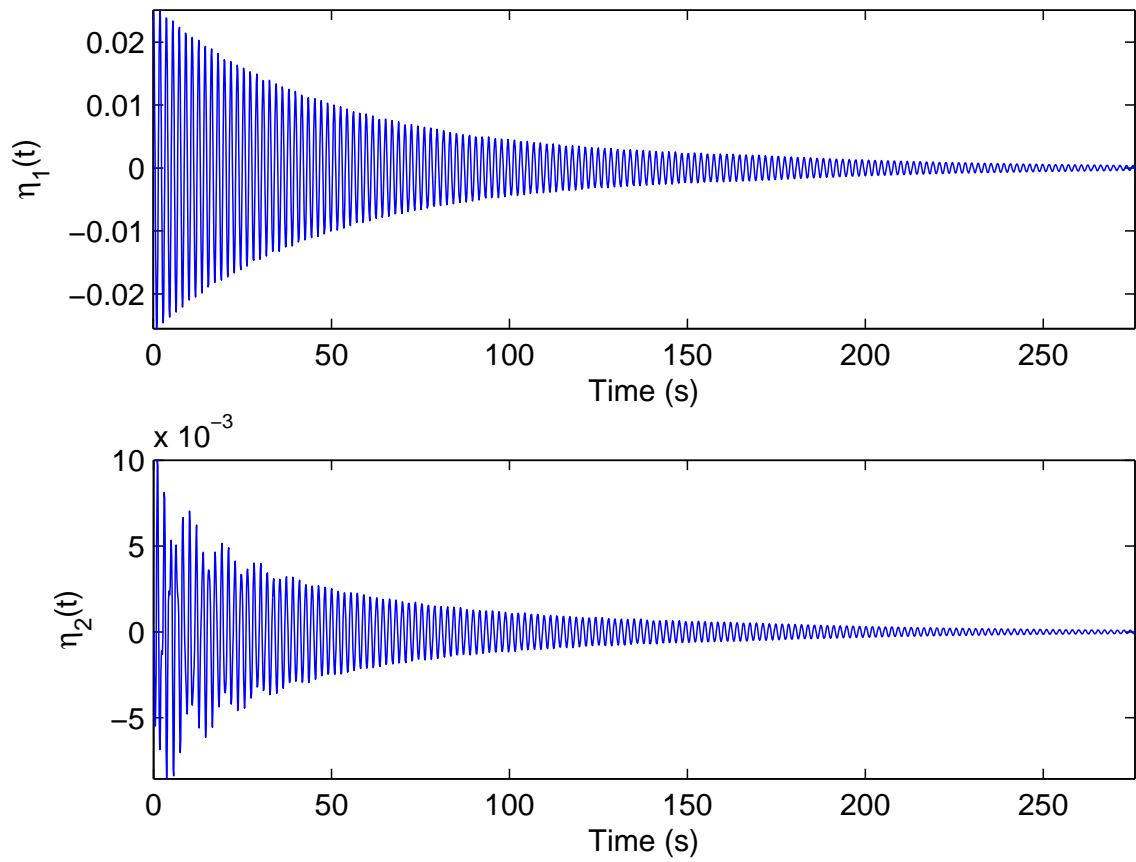
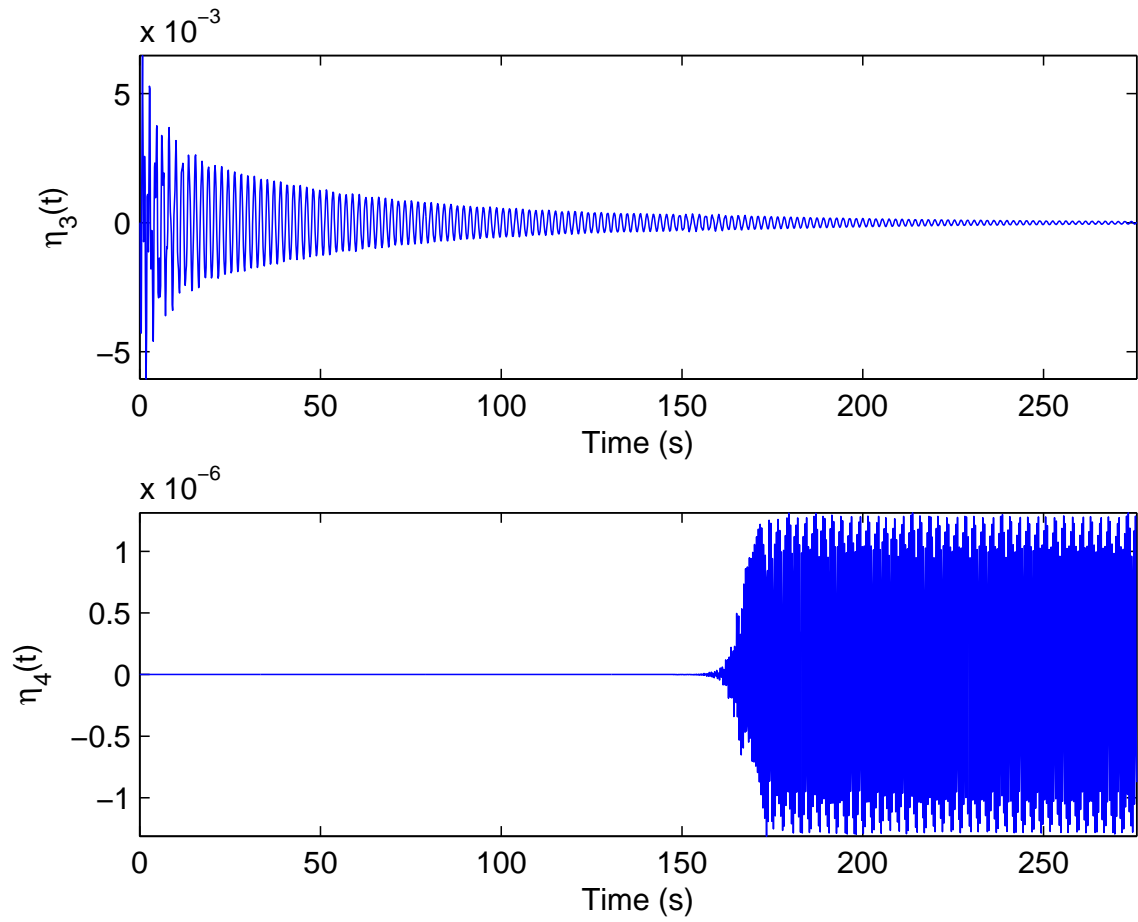Figure 4.2: Uncontrolled lower modes.
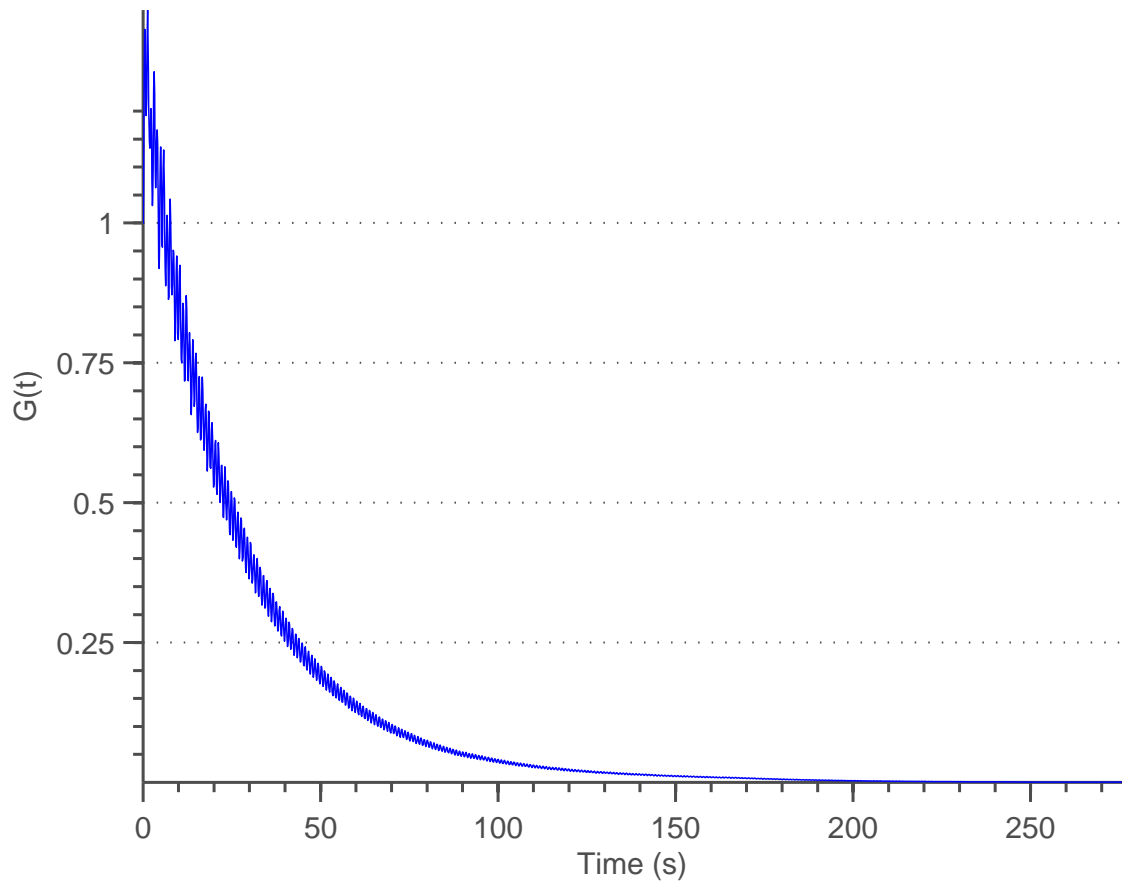
Figure 4.3: Uncontrolled upper modes.

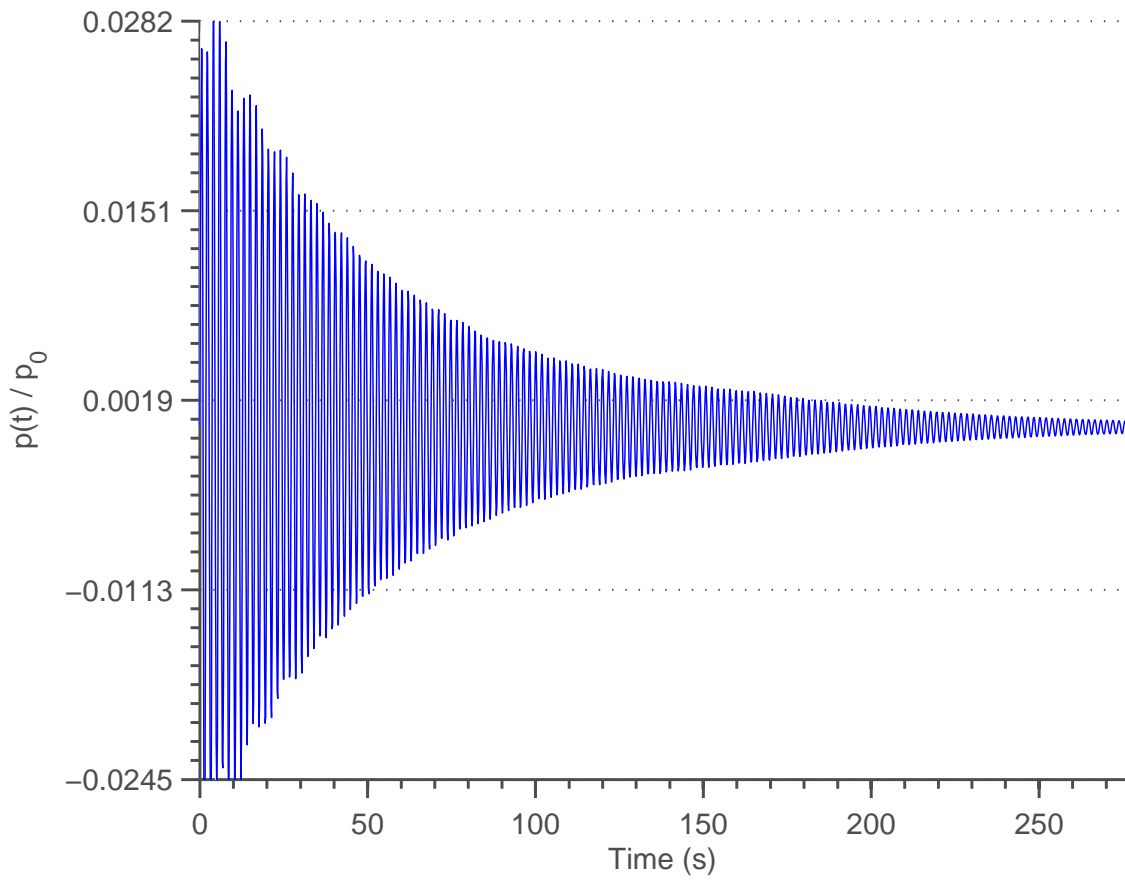Figure 4.4: Energy of an uncontrolled system.

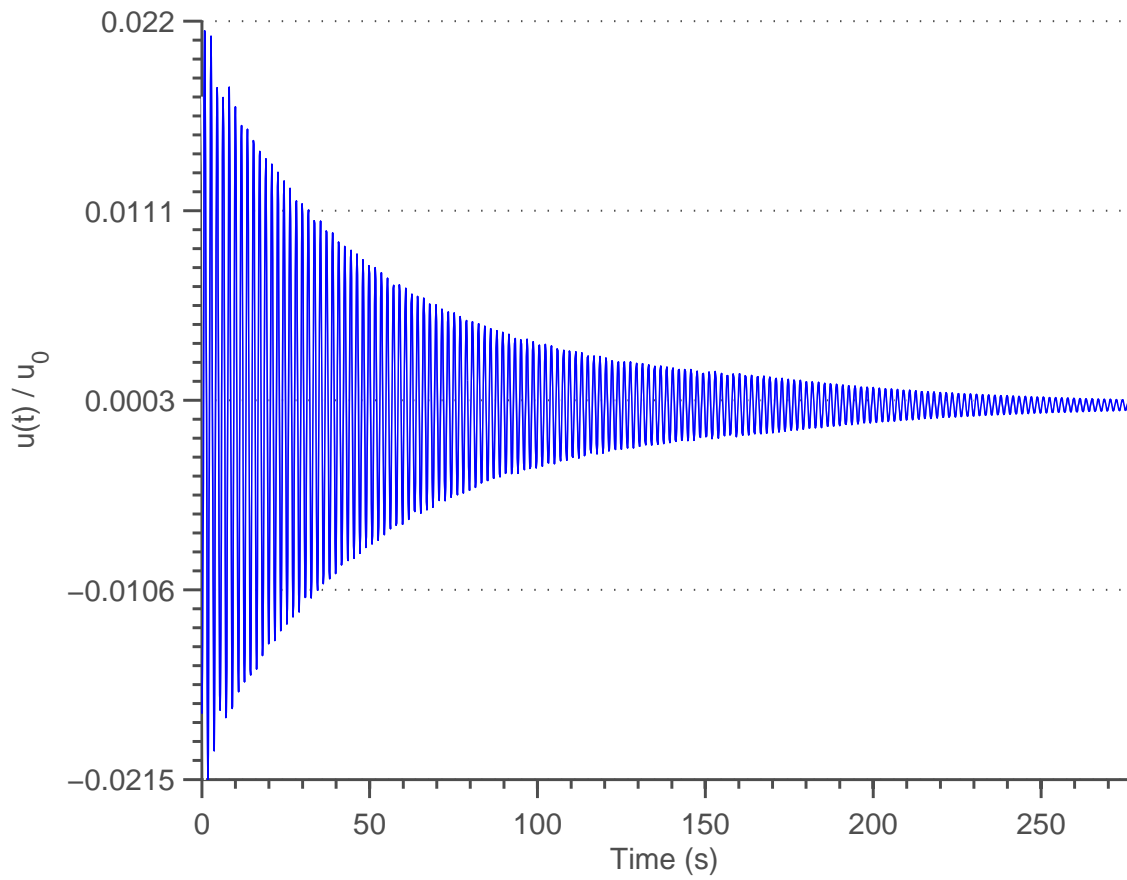Figure 4.5: Pressure disturbance at location of heat source 1.

Figure 4.6: Velocity disturbance at location of heat source 1.

Chapter 5

CONCLUSIONS AND FUTURE

WORK

A thermoacoustic model was constructed based on a Galerkin approximation. The four

lower modes ($j = 1, 2, 3, 4$), were used to simulate the behaviour of the velocity and pres-

sure disturbances, and a thermoacoustic instability was successfully simulated. While the

model is incapable of providing a full representation of the instabilities once these have

reached their maximum energy, it is able to show the initial triggering of the lower modes,

which later propagate the instabilities to the higher frequencies. The main purpose of the

model is to provide an accurate representation during the triggering and stable periods;

which is when the controller is expected to operate. The mathematical model can then be

considered valid under these circumstances.

The development of the controller allowed us to determine the placement of the actu-

ator. These locations have to meet conditions specified in Section 3.1. Additionally, the

converging value of the control parameters $\mathscr{R}_k$ and $\mathscr{S}_k$ was shown to be sensitive to the

location of the actuators, increasing or decreasing performance.

An example of a controller with two actuators was analyzed in detail. The control scheme made the control input U_k limited to the two lower modes. Despite this, the controller proved effective and was partially successful. The triggering in the higher frequency modes is unavoidable in our problem, but stabilizing low frequency disturbances, enough energy is dissipated by natural damping and the controller such that the system becomes stable.

A form of passive control was also studied. We were able to show the impact of the placement of a second heater on the linear term of the heat release. Because our initial disturbance is small, the nonlinear term takes some time to evolve, and any energy exchanged between this term and the linear portion is effectively canceled. Nonetheless, small disturbances in all the frequencies were still present, any deviation on the parameters of the system could effectively lead to triggering. This demands the use of an active nonlinear controller to assure stability.

Currently, the problem does not have an observer. The feedback is provided by the values calculated in the simulation itself. Work regarding the observability of such systems has been previously studied in [Morgans and Dowling (2005)] and [Dowling and Morgans (2005)] and observer designs in a linear system can be found in [J. Rubio-Hervas (2014a)]. Where the heat release is assumed to be known and the heat coefficient $\mathscr{K}_g$ to be constant. In a real-world application this can cause issues due to the unpredictability of convection systems and the variance of the fluid temperature around the heat source; this is specially true when the heater is placed in a node of the natural frequencies of the system. This requires a more complex analysis of the fluid continuity equations.

Appendix A - Simulink Diagram

In order to test the controller on the thermoacoustic system, a Matlab script was used with a simulink code. The script defined the parameters of the environment, while the Simulink code applied the controller. The block diagram can be seen in Figure 5.1.

For the simulink solver, a fixed-step ode4 or Runge-Kutta (RK4) was selected.
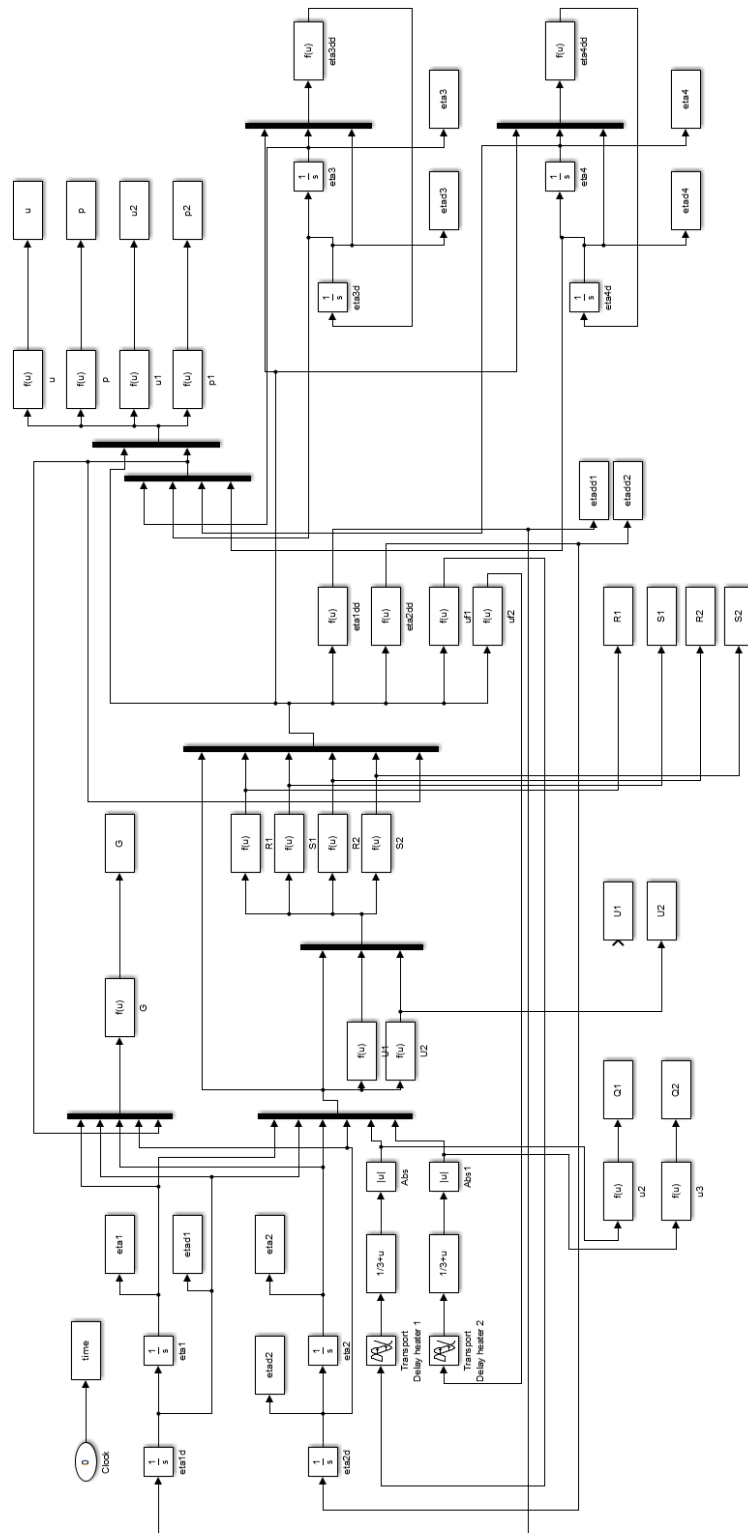
Figure 5.1: Simulink block diagram for nonlinear controller.

Bibliography

A. M. Annaswamy. Thermoacoustic instability: Model-based optimal control designs and experimental validation. *IEEE Transactions on Control Systems Technology*, (333200): 905–918, 2000. doi: 10.1109/87.880593.

S. M. Correa. Power generation and aeropropulsion gas turbines: from combustion science to combustion technology. In *27th Symposium on Combustion*, pages 1793–1807. General Electric Corporate Research and Development Center, 1988.

F. E. C. Culick. Combustion instabilities in liquid-fueled propulsion systems. In *AGARD Conference Proceedings*, volume 450. California Institute of Technology, 1988.

A. P. Dowling and A. S. Morgans. Feedback cojntrol of combustion oscillations. *Annual Review of Fluid Mechanics*, 37:151–182, 2005. doi: 10.1146/annurev.fluid.36.050802. 122038.

J. Epperlein, B. Bamieh, and K. Astrom. Thermoacoustics and the rijke tube: Experiments, identification, and modeling. *Control Systems Magazine*, pages pre–print, 2014. doi: 10.1175/1520-0493.

M. Fleifil. The origin of secondary peaks with active control of thermoacoustic instability. *Combustion Science and Technology*, (133):227–267, 2007.

M. Reyhanoglu J. Rubio-Hervas, D. Zhao. Observer-based control of rijke-type combustion instability. In *AIP Conference Procedings*, volume 1637, pages 899–906. American Institude of Physics, AIP Publishing, 7 2014a.

M. Reyhanoglu J. Rubio-Hervas, D. Zhao. Linear-quadratic-gaussian control of rijke-type combustion instability. *Mathematics in Engineering, Science and Aerospace*, 5(4):1–12, 2014b.

W. Mackunis J. Rubio-Hervas, M Reyhanoglu. Observer-based sliding mode control of rijke-type combustion instability. *Journal of Low Frequency Noise, Vibration and Active Control*, 32(2):201–218, 2015.

C. Ji. Numerical simulation of passive control of self-exited thermoacoustic instabilities by using a secondary heater. *The 21st International Congress on Sound and Vibration*, 2014.

M. P. Juniper. Triggering in the horizontal rijke tube: non-normality, transient growth and bypass transition. *Cambridge University*, (667):272–308, 2010. doi: 10.1017/S0022112010004453.

M. P. Juniper. A theoretical approach for passive control of thermoacoustic oscillations: Application to ducted flames. *Journal of Engineering for Gas Turbines and Power*, 135 (091604-1), 2013. doi: 10.1115/1.4024957.

L. D. Landau and E. M. Lifshitz. *Fluid Mechanics*. 1959.

K. Matveev. *Thermoacoustic Instabilities in the Rijke tube: Experiments and Modeling*. 2003.

A. S. Morgans and A. P. Dowling. Model-based control of a rijke tube combustion instability. *AIAA/CEAS Aeroacoustics Conference*, 2005.

J. Rubio-Hervas, D. Zhao, and M. Reyhanoglu. Nonlinear feedback control of self-sustained thermoacoustic oscillations. *Aerospace Science and Technology*, (41):209–215, 2015.

R. W. Schefer. Hydrogen enrichment for improved lean flame stability. *Science Direct*, (28):1131–1141, 2003.

H. Wang. Numerical solutions of the one-dimensional primitive equations using galerkin approximations with localized basis functions. *Monthly Weather Review*, 100(10):738–746, 1972. doi: 10.1175/1520-0493.

X. Yang, A. Turan, and S. Lei. Nonlinear thermoacoustic in/stability of a rijke tube with a distributed heat source. In *Proceedings of the European Combustion Meeting*. Thermal Management Research Group, 2015.

D. Zhao and M. Reyhanoglu. Feedback control of acoustic disturbance transient growth in triggering thermoacoustic instability. *Journal of Sound and Vibration*, (333):3639–3656, 2014.